

CHARACTERIZATION OF FERROCHROME SMELTER SLAG AND ITS IMPLICATIONS IN METAL ACCOUNTING

by

Makiwe Annette Nkohla

Dissertation submitted in fulfillment of the requirements for the degree Magister Technologiae (M-Tech) in Chemical Engineering, in the Department of Chemical Engineering at the Cape Peninsula University of Technology.

December 2006

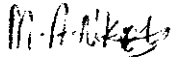
Promoters:

Mr A.B. Nesbitt (Chemical Engineering, Cape Peninsula University of Technology)

Prof. J.J. Eksteen (Process Engineering, University of Stellenbosch)

DECLARATION

I hereby certify that this thesis represents my own work, except where specifically acknowledged in the text. It contains confidential information. This thesis has not previously been submitted for academic examination towards any qualification.



Makiwe Annette Nkohla

December, 2006

SUMMARY

Better metallurgical accounting practices are achieved through implementation of robust and accurate analytical techniques, in particular the sample preparation techniques involved, as well as characterization of all possible errors associated with such techniques and those associated with the characteristics of the materials to be analyzed. As a contribution to the AMIRA P754 project which aims at developing standards and tools for metal balancing, reconciliation and reporting from mine resource to final product, this thesis presents best practices for the characterization of ferrochrome smelter slag. The characterization of the slag is also essential for process control, and thus its implications to the performance of the smelting process are also discussed in this thesis.

Slag samples from a ferrochrome smelter were analyzed using an XRF powder pellet analytical technique in contrast to the ICP technique used at the plant laboratory, to determine their composition. This was done to evaluate the possibility of using XRF as an alternative technique to improve the turnaround times at the plant laboratory. It was found that the XRF analysis of the composite slag by pressed powder pellets could be performed rapidly, but because of the grain size effects resulted from the entrained alloy particles which could not pulverize well, the results were not accurate. This then led to the introduction of an extra stage (oxidation of the entrained alloy particles) in the sample preparation procedure, which prolonged the turnaround time by about 16 hours. However, an important achievement was that the entrained alloy particles could be oxidized into their oxides to obtain homogeneous samples and therefore representative sub-samples. This is an important improvement in the practices at the plant laboratory which involved excluding some of the entrained alloy particles and thus analyzing biased, non-representative samples.

A rapid estimation of the percentage of the entrained alloy in slag was proven to be possible using a simple model (which relates density and the mass fraction of the entrained alloy), in conjunction with a density measuring device (a pycnometer). This ability serves as a significant improvement in the mass balancing and metallurgical accounting practices at ferrochrome producers.

This thesis also describes the manner in which heterogeneity can be quantified as well as the errors associated with heterogeneity and their implications to the analysis results.

Heterogeneity in ferrochrome slag has been found to depend significantly on the amount of alloy entrainment in slag, and therefore the slag viscosity, tapping temperature and chemical composition. One can therefore conclude that the sampling constant and therefore sample mass is dependent on furnace operating conditions.

DEDICATION

This thesis is dedicated to my family for their support, especially my sister, Yandiswa, who has been there with me every step of the way.

ACKNOWLEDGEMENTS

This thesis has been made possible by people who, in various ways, have contributed significantly throughout the course of the project. I therefore would like to thank the following:

- Samancor Chrome (Ferrometals) staff: Shawn Classen, Marius Visser and Willem Smith for their time and effort in making the required information available, and for accommodating our team at the plant. Bert Thompson and his team for accommodating me at the plant laboratory and providing the required information. A special thank you, once again, to Marius Visser for arranging the sampling and delivery of extra samples.
- My co-supervisor at the University of Stellenbosch, Prof. Jacques Eksteen, for his support and guidance. If it was not for his belief in my capability, this thesis would not have been completed.
- My supervisor at the Cape Peninsula University of Technology, Allan Nesbitt, for his help with the academic issues.
- AMIRA P754 for financial support, together with the sponsors:
 - BHP Billiton Ltd
 - Anglo Platinum Ltd
 - Anglo American PLC
 - Kumba Resources Ltd (through Zincor)
 - Rio Tinto PLC
- Elton Thyse for taking samples at Ferrometals plant.
- The staff at the Geology department (University of Stellenbosch): Esmé Spicer for her help with XRF and SEM analysis, and Johnny for his help with the preparation of powder pellets.
- Wezi Banda for helping me with the use of induction and tube furnaces.
- The workshop staff (Process Engineering) for preparing the graphite crucibles.
- Not forgetting the assistants (Process Engineering): Vincent Carolissen, Charles Atkins and James Olin, who were always willing to help.

TABLE OF CONTENTS

1. INTRODUCTION	1
1.1. Brief background	1
1.2. Electric arc chromite smelters	2
1.3. Thermochemistry and metal distributions in reductive chromite smelting	2
1.3.1. Alloy-slag-gas reaction chemistry and mechanisms	3
1.4. Overview of slag handling practices at Ferrometals	5
1.4.1. Tapping and sampling	5
1.4.2. Slag processing for metal reclamation	7
1.4.3. Sample preparation, analysis and associated errors	8
1.5. Problems of major significance to metallurgical accounting	9
1.6. Objectives	10
1.7. Hypotheses	11
1.8. Thesis outline	11
2. LITERATURE REVIEW	12
2.1. Slag properties and their role in smelting operations	12
2.1.1. Slag chemistry	13
2.1.2. Slag viscosity	15
2.1.3. Liquidus temperature	17
2.1.4. Density	18
2.1.4.1. Model(s) for estimating the density of slags	19
2.1.5. Mineralogy	20
2.2. Chemical analysis	22
2.2.1. Sampling and sample preparation	22
2.2.1.1. Sampling error(s)	24
2.2.1.2. Sample preparation errors	24
2.2.2. ICP analysis at Ferrometals	26
2.2.3. Theory of X-ray Fluorescence spectrometer (XRF)	27
2.2.3.1. Sample preparation techniques	27
2.2.3.2. Calibration and matrix effects	29
2.3. Mineralogical analysis	31
2.3.1. Image analysis	31
2.3.2. Scanning Electron Microscope (SEM) images	31

2.4. Heterogeneity.....	33
2.4.1. Estimation of the relative variance of the fundamental error, σ^2	33
2.4.2. Sampling Constant – definition and use	37
3. RESEARCH METHODOLOGY	39
3.1. Slag chemical characterization	39
3.1.1. Standards preparation	39
3.1.1.1. Reagents used.....	39
3.1.1.2. Method	40
3.1.2. Sample preparation	41
3.1.3. Calibration and analytical conditions	42
3.2. Density and entrained alloy characterization.....	43
3.3. Heterogeneity characterization	44
3.3.1. Estimation of size distributions.....	44
3.3.1.1. Sample preparation	44
3.3.1.2. Size analysis.....	45
3.3.2. Separation into density distributions.....	45
4. RESULTS AND DISCUSSION.....	46
4.1. Chemical characterization of slag.....	46
4.2. Characterization of entrained alloy in slag	49
4.3. Heterogeneity quantification	51
4.3.1. Size distribution(s) of entrained alloy in slag	52
4.3.2. Estimation of sampling constant and Relative standard deviation	53
5. CONCLUSIONS AND RECOMMENDATIONS.....	57
6. REFERENCES	60
7. APPENDIX A: RESULTS AND SAMPLE CALCULATIONS	64
7.1. XRF results	64
7.2. Calculation of alloy entrainment in slag.....	66
7.3. Calculation of the sampling constant and RSD, %.....	67
8. APPENDIX B: SEM BSE IMAGES OF SLAG	73
9. APPENDIX C: SAMPLING METHODS.....	77
9.1. Sectorial Splitter	77
9.1.1. Advantages of a sectorial splitter.....	77
9.2. Incremental sampling.....	78
9.3. Riffle splitting.....	79

9.4. Alternate shovelling.....	81
9.5. Coning and quartering	81
9.6. Rolling and quartering	82
9.7. Fractional shovelling	83
9.8. Degenerate fractional shovelling	84
9.9. Table sampler.....	85
9.10. V-Blender	85
9.11. Vibratory spatula	86
9.12. Grab sampling.....	86

LIST OF FIGURES

Figure 1. 1: Schematic of the inside of the submerge-arc furnace during smelting (Riekkola-Vanhanen, 1999).....	1
Figure 1. 2: An SEM photo of a section of polished bulk slag sample	6
Figure 2. 1: Chromium content in slag as a function of the basicity in the system Ca-Mg-Fe-Cr-Si-O at 1600 °C (Muan, 1984).....	14
Figure 2. 2: Change in viscosity of slags after additions of CaO, Fe ₂ O ₃ and Cr ₂ O ₃ (Rennie, Howat and Jochens, 1972).....	17
Figure 2. 3: System MgO-Al ₂ O ₃ -SiO ₂ ; composite	18
Figure 2. 4: Ferrochrome smelting slag at 1600 °C containing non-dissolved PAC (Hayes, 2004).....	21
Figure 2. 5: Ferrochrome smelting slag “slow cooled” from the furnace showing the precipitation of secondary spinel (Hayes, 2004).....	21
Figure 2. 6: Typical slag processing at laboratory.....	23
Figure 2. 7: Calibration curve for Cr in a FeCr alloy (Willis, 2004).....	30
Figure 2. 8: Calibration plots for Fe in stainless steel (Willis, 2004).....	30
Figure 2. 9: Example of a BSE image	32
Figure 3. 1: Schematic diagram of the tube furnace set-up (Banda, 2001)	40
Figure 3. 2: Pressed powder pellet	42
Figure 4. 1: FeO concentration in various slag samples.....	47
Figure 4. 2: Relationship between slag density and the amount entrained.....	50
Figure 4. 3: Size distributions of alloy particles in ferrochrome slag.....	52
Figure 4. 4: BSE image showing entrained alloy particles	53
Figure 4. 5: Sampling constant for samples from five consecutive taps	55
Figure 8. 1: T4A (1, 2, 3), T4B (4, 5, 6, 7, 8).....	73
Figure 8. 2: T1A (1, 2, 3, 4), T1B (5, 6, 7, 8).....	74
Figure 8. 3: T2B (1), T2C (2, 3, 4), T2A (5), T3B (6, 7), T3C (8).....	75
Figure 8. 4: T5A (1, 2, 3), T5B (4, 5, 6).....	76
Figure 10. 1: A sectorial splitter with eight sectors.....	77
Figure 10. 2: Top (increments selected with an incorrect device), Bottom (increments selected with a correct device).	78
Figure 10. 3: A riffle splitter with 20 chutes and two collection pans	80
Figure 10. 4: The alternate shoveling procedure	81

Figure 10. 5: The coning and quartering procedures.....	82
Figure 10. 6: The fractional shoveling procedure.....	83
Figure 10. 7: The degenerate fractional shoveling procedure	84
Figure 10. 8: A table sampler	85
Figure 10. 9: A V-blender	86

LIST OF TABLES

Table 2. 1: Recommended values for partial molar volume \bar{V} of various slag constituents at 1500 °C (Keene and Mills, 1995)	20
Table 3. 1: Content range of each component in standard samples	41
Table 3. 2: Analytical conditions.....	43
Table 4. 1: Comparison of results of XRF and ICP	48
Table 4. 2: Alloy entrainment in various slags (non-alloy slag density = 2.98 g/cm ³)	49
Table 4. 3: Constitutional heterogeneity for sample t3, a _L = 8.63 %	53
Table 4. 4: Constitutional heterogeneity (size factors), t3.....	54
Table 4. 5: Sampling constants and relative errors for five consecutive taps	55
Table 7. 1: XRF results of oxidized slag	64
Table 7. 2: XRF results of non-oxidized slag, metallic particles selected out	65
Table 7. 3: XRF results of slag pulverized with metal droplets	66
Table 7. 4: Constitutional heterogeneity (density factors) for sample t5, a _L = 9.72 %	68
Table 7. 5: Constitutional heterogeneity (size factors), t5.....	69
Table 7. 6: Constitutional heterogeneity (density factors) for sample t2, a _L = 11.85 %	69
Table 7. 7: Constitutional heterogeneity (size factors), t2.....	70
Table 7. 8: Constitutional heterogeneity (density factors) for sample t1, a _L = 10.42%	70
Table 7. 9: Constitutional heterogeneity (size factors), t1.....	71
Table 7. 10: Constitutional heterogeneity (density factors) for sample t4, a _L = 10.06 %	71
Table 7. 11: Constitutional heterogeneity (size factors), t4.....	72

GLOSSARY OF TERMS

Slag: High temperatures melt of inorganic oxides (derived from minerals) that may contain entrained metal or alloy droplets and non-dissolved minerals. Slags are normally studied once they are quenched (fast-cooled) and solidified.

Ferrochrome: The alloy formed when natural chromite mineral is reduced, in the presence of fluxes (which reduce the mixture melting point) with carbonaceous reductant such as coal, anthracite, coke or char. Its main components are: Cr-Fe-C-Si in decreasing order of concentration. Ferrochrome is one of the major ingredients for the manufacture of stainless steels.

Metal Accounting: The system whereby selected process data (pertaining to metals of economic interest) is collected from various sources including mass measurement and analysis and transformed into a coherent report format that is delivered in a timely fashion in order to meet specified reporting requirements.

Metallurgical (Metal) balance: The determination (through measurement and analysis), and computation of the magnitude of each component of interest across an entire process or across each section of a process flow sheet. A metallurgical balance, which is suitable for reporting of Metal Accounting, should be supplemented by defined uncertainties associated with each determination.

XRF: X-ray Fluorescence spectrometry (instrumental analytical technique).

ICP: Inductively Coupled Plasma (instrumental analytical technique).

SEM: Scanning Electron Microscope

BSE: Backscattered Electron (type of image produced during SEM analysis)

SE: Secondary Electron (type of image produced during SEM analysis)

RSD: Relative Standard Deviation

PAC: Partially Altered Chromite

PPP: Pressed Powder Pellet (a specimen produced by pressing a powder sample into a pellet, for analysis by XRF)

FGB: Fused Glass Bead (a specimen produced by fusing a powder sample in a borate flux, and casting it into a pill-like glass, for analysis by XRF).

1. INTRODUCTION

1.1. Brief background

Ferrochrome is the major chromium source for use as the main raw material for stainless steel production, and Ferrometals is one of the largest ferrochrome alloy producers in the world. Submerged-arc furnaces are most commonly utilised to smelt chromite ores by using suitable carbonaceous reductants such as coke, bituminous, char, etc. During the smelting process slag is created and metallic ferrochrome coalesces into droplets, which being the heavier phase, separate out of the slag by settling through the slag to the bottom of the furnace (Figure 1.1).

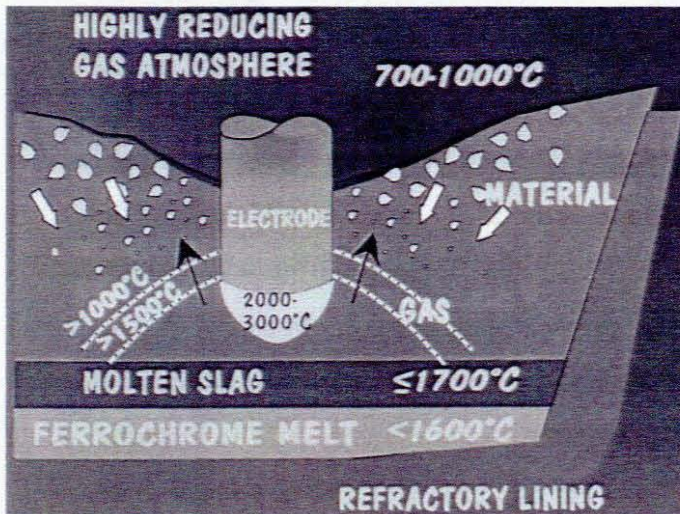


Figure 1. 1: Schematic of the inside of the submerge-arc furnace during smelting (Riekkola-Vanhanen, 1999)

Ferrochrome slag consists mainly of SiO_2 , Al_2O_3 and MgO in different proportions but also smaller amounts of CaO , chromium and iron oxides, with significant quantities of chromium in the form of PAC and entrained alloy (Hayes, 2004). The amount of chromium in slag is much influenced by the slag composition, temperature and the tapping arrangement. The role of the slag in the process is thus essential and specific chemical, physical and mineralogical properties are required not only for process monitoring, but also for metallurgical accounting. For metallurgical accounting, utilization of the best practices available to obtain reliable (accurate and precise) data is essential, be it chemical, physical or mineralogical data. The reason for this is that mass balances are done to calculate the amounts of ferrochrome alloy

and slag produced, based on the slag and alloy analysis. The laboratory techniques for obtaining these data usually involve sampling and sample preparation processes, for which utilization of the best practices is also essential, such that errors introduced by these processes are kept at minimum levels. The techniques utilized should also allow rapid turnaround times so that any deviations in the process can be detected and rectified as soon as possible.

At the moment good metal accounting practice at ferroalloy producers (using submerged-arc furnace technology) is seriously hampered by biases, poor representativity of samples and very slow information turnaround times, based on the laboratory practices (Bartlett, 2003).

Before the characterization techniques of slags are investigated, it is sensible to look at the production processes that produce these slags to obtain some understanding at the sources of the various slag components, and its physical and chemical behaviour.

1.2. Electric arc chromite smelters

Ferrochrome is typically produced in South Africa from chromite in either a submerged arc or open arc furnaces (DC plasma). Chromite is a spinel mineral and forms part of the spinel crystal family, having the general formula: $(\text{Fe}^{2+}, \text{Mg}^{2+})\text{O} \cdot (\text{Al}^{3+}, \text{Cr}^{3+}, \text{Fe}^{3+})_2\text{O}_3$. The raw material particle size requirement and reductant requirement are significantly different, as the submerged arc furnaces require a porous burden with a narrow range of electrical conductivity and a reductant of high strength, while the open arc furnaces are not constrained in this way. Open arc furnaces can therefore treat chromite fines and operate with low-strength, high rank coals such as anthracite of reasonably small particle size (1 - 20 mm). A number of ferrochrome producers are to be found in the central-southeast Bushveld complex, where a combination of high alloy steel producers (Highveld Steel and Vanadium and Columbus Stainless Steel), the availability of coal, inexpensive electrical power and chromite create an area of industrial synergism.

1.3. Thermochemistry and metal distributions in reductive chromite smelting

During the reductive smelting of chromite in an electric arc furnace, chromite is reduced, in the presence of flux (quartz) to a low Cr_xO slag and high carbon ferrochrome (HCFerCr) alloy.

A typical (major component) composition of the chromite, slag and alloy are as follows, based on ICP analysis:

Chromite (lumpy): 14.49% Al_2O_3 , 1.08% CaO , 39.51% Cr_2O_3 , 23.45% Fe_2O_3 , 10.65% MgO , 8.32% SiO_2 .

Slag: 24.69% Al_2O_3 , 2.98% CaO , 18.61% Cr , 10.65% Fe , 19.83% MgO , 23.24% SiO_2 .

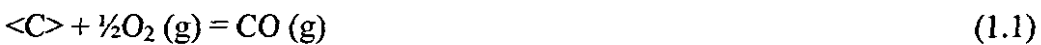
Alloy: 51.25% Cr , 36.35% Fe , 3.63% Si , 6.79% C , 0.17% Mn , 0.018% P , and 0.029% S .

The analysis given above is as-reported, meaning that it does not necessarily reflect the true oxidation states of the metals, especially with regards to the metals Fe and Cr , which exist in a number of oxidation states. Moreover, the slag analysis includes entrained alloy droplets which cannot be thermodynamically predicted – their mechanical entrainment is determined more through the rheological properties of the slag than through thermochemical behaviour. If it is assumed that the chrome and iron exists primarily as entrained droplets, then the dissolved Cr and Fe becomes relatively insignificant relative to the other major slag components. If the entrained Cr and Fe are therefore subtracted and the compositions renormalized, the slag take on the following composition with respect to the major components: 34.90% Al_2O_3 , 4.13% CaO , 28.03% MgO , 32.85% SiO_2 . However, this remains an oversimplification as non-dissolved partially altered chromites (PACs) remain in the slag (Cr^{3+}). The amount of PACs becomes the main form of Fe and Cr losses in submerged arc furnaces as the slow dissolution of the lumpy ore types used limits complete dissolution.

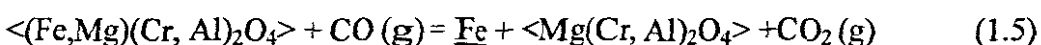
1.3.1. Alloy-slag-gas reaction chemistry and mechanisms

Barcza *et al.* (1981) proposed a possible smelting reaction mechanism of chromium ore fines and fluxes at 1600 °C, and classified the reaction in various reaction groups:

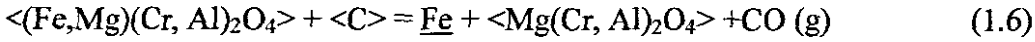
Group I (Control of the p_{O_2} in the gaseous phase):



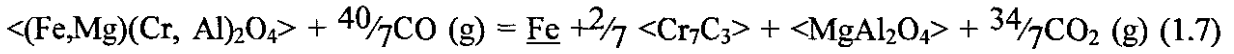
Group II (Solid state reductions on the surface of the bath - Iron oxide reduction becomes feasible at p_{O_2} of less than 10^{-5} atm):



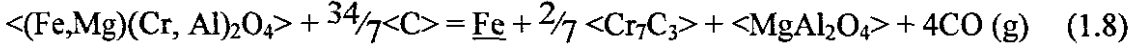
Or



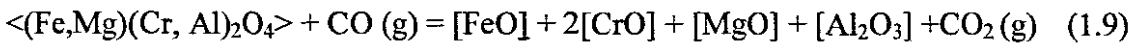
The reduction of chromium oxide becomes feasible at a p_{O_2} of less than 10^{-7} atm:



Or



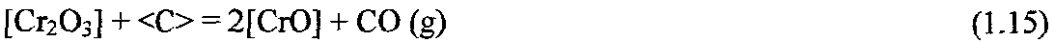
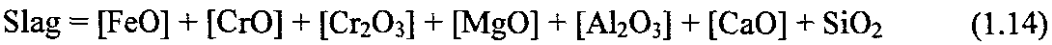
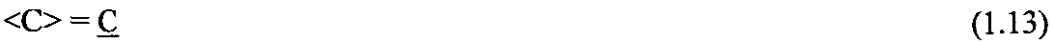
Group III (Dissolution of the chrome spinel in the slag phase at p_{O_2} of less than 10^{-8} atm):



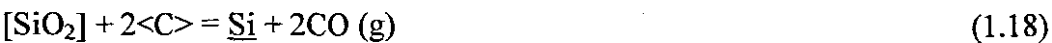
Or



Furthermore:



Group IV: Reduction reactions

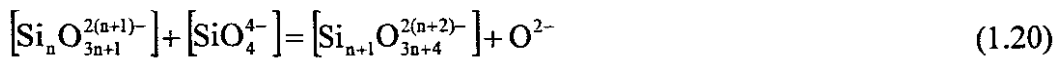


Acid-base reaction in the slag (simplified):

Metal oxide ionisation reactions, for example:



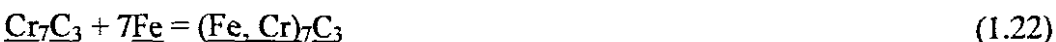
Polymerisation / depolymerization reactions:



And,



Alloy formation:



In the above equations, “<>” refers to the solid phases, “_” refers to the alloy phase and “[]” refers to the slag phase. Barcza *et al.* (1981) noted that the reactions in a pilot scale furnace proceeded extremely fast and that well reduced slags (Cr_2O_3 below 5%) were tapped from the furnace 5 minutes after the feed has been shut off. Two major reaction mechanisms were proposed, one in which the (solid state reduction) the spinel retains its form (Mechanism A), whereas in the other, the entire spinel dissolves (Mechanism B). Mechanism A, while contributing slightly to the overall reduction of chromite was observed to be too slow to account for the actual conversion. Mechanism B becomes favourable under very low oxygen partial pressures (as stated earlier, the solubility of chromite in the slag is very dependent on the oxygen partial pressure, its solubility increasing with reducing $p\text{O}_2$). As the approach of equilibrium via gas-liquid reactions is relatively slow, it is unlikely that the gas phase will control the oxygen activity in the slag system under consideration. Barcza *et al.* (1981) therefore show that the metal phases present, especially chromium and silicon, have a far greater controlling influence on the oxygen activity in the slag. They also show that there is a strong relationship between Si in the metal and the Cr_2O_3 content of the slag. As silicon is reduced from silica in the slag with carbon (also carbon dissolved in the alloy), the solubility of Cr_2O_3 in the slag is therefore inherently dependent of the carbon addition: The lower the oxygen activity (due to carbon addition), the larger is the Cr^{2+} -to- Cr^{3+} ratio and therefore the greater the solubility of chromium oxide in slag. On the other hand, they have shown that the dissolution and reduction of iron is possible at higher oxygen partial pressures, leading to residual, altered, but virtually non-dissolved spinel particles, with almost no iron oxide remaining.

1.4. Overview of slag handling practices at Ferrometals

Six submerged-arc furnaces produce ferrochrome through the carbothermic reduction of chromite ore. The furnaces operate on a 3 shift basis, and the products, ferrochrome alloy and slag are tapped 3 times per shift at intervals of approximately 2.5 hours between taps.

1.4.1. Tapping and sampling

The tapping arrangement at Ferrometals is cascade tapping which means that slag and alloy are tapped together (from the same taphole) into two ladles in series. The lower density slag floats at the top and eventually overflows from the first ladle into the second ladle and then

down to the break floor. During each tapping process, slag samples for analysis are taken by immersing a cold steel pipe into the molten slag after it has been tapped into a ladle from the furnace (thus, a total of three samples are taken on a shift). Once the slag has solidified and cooled it is put into a sample bag and delivered to the plant laboratory where it is analyzed by Inductively Coupled Plasma (ICP) spectrometry technique to determine its chemical properties. A typical “snapshot” of a polished section of slag tapped from the furnace is shown by the Scanning Electron Microscopy (SEM) photograph in Figure 1.2.

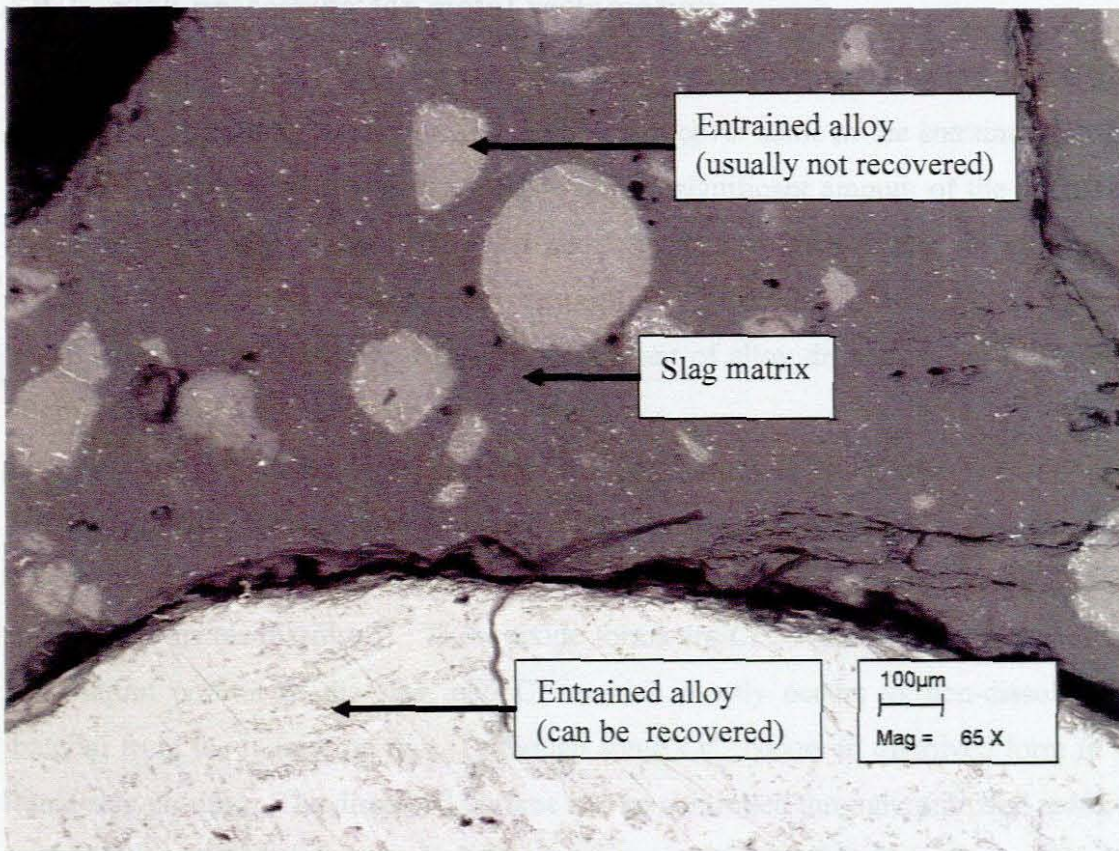


Figure 1. 2: An SEM photo of a section of polished bulk slag sample

This specific slag sample derived from a stage when the furnace experienced upset conditions which lead to severe alloy entrapment in the slag, as is visible from the size of the alloy droplet at the bottom of the photomicrograph.

Losses of metal to slag are apparent with a significant amount of alloy droplets occurring in the size range $30\mu\text{m} - 2000\mu\text{m} / 2\text{mm}$, some ($>1\text{mm}$) can be recovered and the remainder ($<1\text{mm}$) cannot (Figure 1.2). Metal losses to slag can occur throughout the reduction process in the furnace, as well as during the tapping and can be attributed to various reasons including:

- Physical entrapment (*entrained alloy losses*) of alloy droplets in the case of their settling through the slag, where very viscous slags may entrain so much alloy that no clear separation between alloy and slag is possible.
- Chemical / electrochemical dissolution (*dissolved chromium and iron in slag*).
- Reactions between the gases and the solid chromite in the furnace may result in the partial reduction of the chromite (*partially altered chromite losses - PAC*).

1.4.2. Slag processing for metal reclamation

The slag from the break floor, once cooled down, is further treated on the reclamation plant comprising of crushing, screening and jiggging, to recover some of the entrained metal. It was originally thought that this plant would recover a significant amount of the entrained alloy. However, as it only recovers entrained alloy droplets of sizes $+2\text{mm}$, it was realized that much of the entrained metallic alloy remains locked in the solidified slag matrix. It is apparent from Figure 1.2 that a significant amount of alloy droplets occur in the size range $30\mu\text{m} - 2000\mu\text{m}$ (or -2mm).

Knowledge-based management to reduce chrome losses to slag would be feasible if it is clear how much chrome is lost to entrained alloy, and how much is present in the alloy-free slag in its oxide forms (as dissolved). These oxide forms are Cr^{2+} which mostly is dissolved in the fully liquid portion of the slag, and Cr^{3+} which mostly occurs as non-dissolved residual material from the lumpy ore types (although some Cr^{3+} occurs in dissolved form in the fully liquid slag portion). The dissolved chrome can be controlled through improved redox-basicity control, while the amount of entrained chrome can be controlled through control of the slag viscosity. To achieve these, quick estimates of the slag composition are required because the slag fluidity and chemistry are strongly related and so, these two components cannot be treated or controlled separately. However, a small change in the slag temperature (based on specific energy input) would have a much larger effect on slag viscosity (and therefore entrainment) than on the redox behaviour.

Cr, Fe and Si are typically reported as total amounts based on laboratory (chemical) analysis of the slag. The oxidation state is therefore unknown and the amount of entrainment is unknown. This could be rectified, as the pure alloy has a known density that does not vary significantly with composition, and the density of the alloy-free slag is also fairly insensitive

to slag chemistry. Furthermore, the alloy density is more than double the slag density, making the estimation of the percent entrained alloy fairly simple, if the density of the bulk composite slag (as tapped) has been measured (i.e. using a very affordable pycnometer). Subtraction of the entrained portion from the bulk slag would allow the calculation of the chemistry of the alloy-free slag.

1.4.3. Sample preparation, analysis and associated errors

As mentioned above (section 1.1.1) three slag samples and three alloy samples taken on a shift are submitted to the plant laboratory, where only one slag and one alloy sample (from the first tap) were analyzed due to work pressure and long sample preparation times, including the time required to bring the samples into solution for ICP analysis. Samples taken from the second and third taps were not analyzed, unless the analysis results of the first tap deviates much from a certain specified value. However, this situation has improved as a result of the suggestions made since the original study, and all samples are currently measured. Sample preparation includes crushing, pulverizing, taking a 0.2 g sub-sample and dissolving it in nitric acid. The coarsely crushed slag sample is inspected and any metal entrapped in the slag is selected out by hand, before pulverizing. This practice is non-sensible as unknown biases are introduced. Moreover, much of the entrained alloy is anyway not removed as it is too small.

The fact that not all samples tapped were analyzed restricted the ability of the metallurgists to identify and rectify deviations in the process to minimize alloy losses to slag, which can be achieved if all the taps are analyzed. Moreover, the amount of slag produced is estimated based on an alumina (Al_2O_3) balance, which is sensible, if it can be assumed that the slag analysis is correct, and if all samples tapped are analyzed. However, because of non-representative sub-sampling resulting from the fact that other particles are selected out before the slag is processed further for analysis, there exist an uncertainty as to the accuracy of the analysis results.

In addition to the problem of non-representative sub-sampling due to biased samples, obtaining representative sub-samples may also be difficult if the material being sampled is heterogeneous, and this may increase the total analysis variance. Referring back to Figure 1.2 again, it is evident that the ferrochrome slags are heterogeneous, as they may have metal or

alloy inclusions. In most cases, because the materials are pulverized prior to weighing the analysis sub-sample, it is often assumed that the errors associated with heterogeneity are negligible, the assumption which in many cases is untrue. So far, no attempts are made at the plant laboratory to evaluate errors of this type and thus their influence is unknown. For metallurgical accounting, it is important that all types of errors be evaluated so that attempts can be done to minimize their effect or at least be accounted for, if they cannot be minimized. Models such as Pierre Gy's sampling theory could be utilized for this purpose (Pitard, 1993).

1.5. Problems of major significance to metallurgical accounting

Following the discussion in the previous sections, a few aspects of major significance to metallurgical accounting have been identified to be problematic at the plant laboratory:

- Due to the overly long sample preparation times associated with ICP analysis, not all samples from available taps were analyzed. Moreover, a small analysis sample of 0.2g could result in severe biases due to non-representativity of samples, for example, in a situation where there could be particles of ferrochrome in the slag. An X-ray Fluorescence spectrometry (XRF) analytical technique could save a significant amount of sample preparation time as it uses pulverized samples pressed into pellets. Furthermore, this technique uses an analysis sample mass as large as about 8g compared to a 0.2g used for ICP, which then resolve (reduce) the uncertainties based on representativity of the samples. However, errors due to heterogeneity need to be characterized.
- Due to non-representative sub-sampling in the laboratory, associated with the fact that not the full aliquots that came from the plant are processed (but only the best appearing pieces from the crushed product), the analysis results are not accurate. Thus, the removal of the entrapped material during sample preparation leads to biased samples, which in turn leads to incorrect mass balances.
- The non-recoverable metal losses remain unaccounted for, as the chemical analysis gives the total amounts of Cr and Fe, and does not indicate whether these are in the alloy form or their oxide forms. The impact of this is important as it influences the reported and interpreted concentration of the other slag species, and therefore also alumina, on which the slag production is based and the metal loss is evaluated. The decisions made to minimize metal losses to slag can also be influenced, for instance, if the reported level of Cr in the slag is high due to entrained rather than dissolved losses, increasing the reducing

conditions to obtain better alloy yield would be worthless, but better control of the slag basicity and temperature would yield improved results.

1.6. Objectives

Better process control and metallurgical accounting practices are achieved through implementation of robust and accurate analytical techniques, in particular the sample preparation techniques involved, as well as characterization of all possible errors associated with such techniques and those associated with the characteristics of the materials to be analyzed. Based on the problems identified with regards to the ferrochrome slags and their analysis, as discussed in the previous sections, this thesis is intended to achieve the following objectives:

- To investigate if an accurate, robust and precise technique could be developed for ferrochrome slag (and alloy) analysis, and if this alternative technique would allow rapid turnaround times of samples analysis.
- To investigate if a density based method could be used in conjunction with a simple robust model, to estimate the amount (%) of entrained metal in slag. The ability to estimate this amount will help improve mass balancing and metallurgical accounting practices at ferrochrome producers.
- To quantify errors associated with the heterogeneity of ferrochrome slags so that the contribution of these errors to the overall sampling and analysis variance is understood. This would aid the smelter to discern if the errors result from poor mixing in the process, or due to sampling, or due to analysis.

The achievement of the above-mentioned objectives would play a significant role in achieving some of the goals of the AMIRA P754 project, of developing standards and tools for metal balancing, reconciliation and reporting from mine resource to final product.

1.7. Hypotheses

The following hypotheses will be evaluated:

- That XRF is a practical and accurate alternative to ICP analysis.
- That pycnometric characterization provides a rapid and accurate method for determination of alloy entrainment.
- That heterogeneity, which is used to determine sample size for a given RSD, is dependent on slag chemistry.

1.8. Thesis outline

Chapter 2 emphasizes the importance of slag characterization by discussing the influence of slag composition to other properties of the slag and therefore the performance of the smelting process. Chemical and mineralogical characterization techniques as well as error quantification techniques are discussed.

Chapter 3 details the sample preparation and analysis procedures followed, as well as the equipment used.

Chapter 4 presents and discusses the important results obtained by the methods described in chapter 3, and long tables and calculations relating to this chapter are included in the appendix. Following this chapter are conclusions and recommendations drawn based on the results.

2. LITERATURE REVIEW

This chapter serves as the platform to the work done which is discussed in the subsequent chapters. The relevant literature on the subject of this thesis has been found to be very limited. Thus, the chapter does not relate much to the work that has been done by other authors but only the work done at the plant laboratory. However, few relevant papers have been found and, information from books and course notes is used where necessary. In this chapter, the properties of the slag produced during ferrochrome production process and their influence in the process efficiency are discussed. Characterization techniques including chemical, mineralogical and error quantification as well as sample preparation techniques are discussed.

2.1. Slag properties and their role in smelting operations

“In ferrochrome process, the slag is a reactive medium, where reduction takes place. The slag dissolves chromite pellets or lumpy ore until at the saturation point and chromium oxide is reduced by carbon to form metallic ferrochrome. Metallic ferrochrome coalesces into droplets, which as a heavier phase, is separated out of slag and settles at the bottom of the furnace”. (Forsbacka and Holappa, 2004).

In order to obtain the right metal analysis, good metal recovery and satisfactory furnace operation, the slag needs to have the following properties:

- The right melting point for the actual metal quality.
- A viscosity enabling easy tapping.
- A good separation between slag and metal.

Thus, during the reduction of the chromite ore, the slag properties have a big influence on the reduction rates (Jansson A., Brabie, Fabo and Jansson S., 2002), with the reduction rate strongly dependent on the composition of the molten slag.

In this section, viscosity and other properties that influence the performance of ferrochrome process such as slag chemistry, liquidus temperature, density, electrical conductivity, are discussed.

2.1.1. Slag chemistry

Ferrochromium slags mainly solidify as a mixture of a glass phase spinel, $MgO \cdot Al_2O_3$ and forsterite, $2MgO \cdot SiO_2$, and will also contain between 3 and 15 % Cr_2O_3 , mainly as unreduced or partly reduced ore, and a small amount of CaO (Riekkola-Vanhanen, 1999).

The chemistry / composition of slag, in particular the slag basicity in ferrochrome production via chromite smelting, is an important factor that affects the distribution of chromium between the metal and the slag. Typical bulk composition of slags in the production of high carbon ferrochrome is in the following ranges:

SiO_2 15 – 30%, typically 23%

Al_2O_3 19 – 33%, typically 25%

MgO 13 – 25%, typically 20%

CaO 1 – 5%, typically 3%

Fe 1 – 12% (may be as FeO or as entrained ferrochrome alloy), typically 8%

Cr 1 – 18% (may be as CrO, Cr_2O_3 or entrained ferrochrome alloy), typically 12%

And, ferrochromium slag basicity is generally expressed as (Muan, 1984. Eksteen, 2003):

$$\frac{\text{mass \% CaO} + \text{mass \% MgO}}{\text{mass \% SiO}_2} \quad (2.1)$$

The following three important slag properties are results of the composition of the slag:

- **Slag viscosity**, which determines physical separation and recovery of metal from slag. High viscosity slags can cause foaming problems in furnace operation.
- **Slag resistivity**, which helps to determine electrode penetration and power input to the furnace with more resistive slags allowing deeper penetration, higher voltage operation and greater power inputs.
- **Slag liquidus**, which determines overall operating temperatures and degree of superheat to the melt.

To optimize the slag composition, other minerals (fluxes) than chromium ore have to be added to the feed burden. The main slag additives (fluxes) used at Finnish Outokumpu are quartzite, aluminium oxide containing material to compensate for the high magnesium content in certain ores, and magnesium and calcium oxide containing material for aluminium rich ores

(Riekkola-Vanhanen, 1999). At Ferrometals, the main slag additives used are quartz (SiO_2) and dolomite ($\text{CaMgCa}(\text{CO}_3)_2$) – for aluminium rich ore.

The effect of slag basicity and other slag components on chromium distribution between metal and slag or to be more specific on chromium losses to slag has been reported by few authors (Muan, 1984. Hollappa and Xiao, 2004). Muan has studied the effect of slag basicity at a constant temperature of $1600\text{ }^\circ\text{C}$ and approximately constant chromium content of the alloy phase (16 – 18 mass %). Figure 2.1 shows the chromium contents as a function of slag basicity resulting from his work.

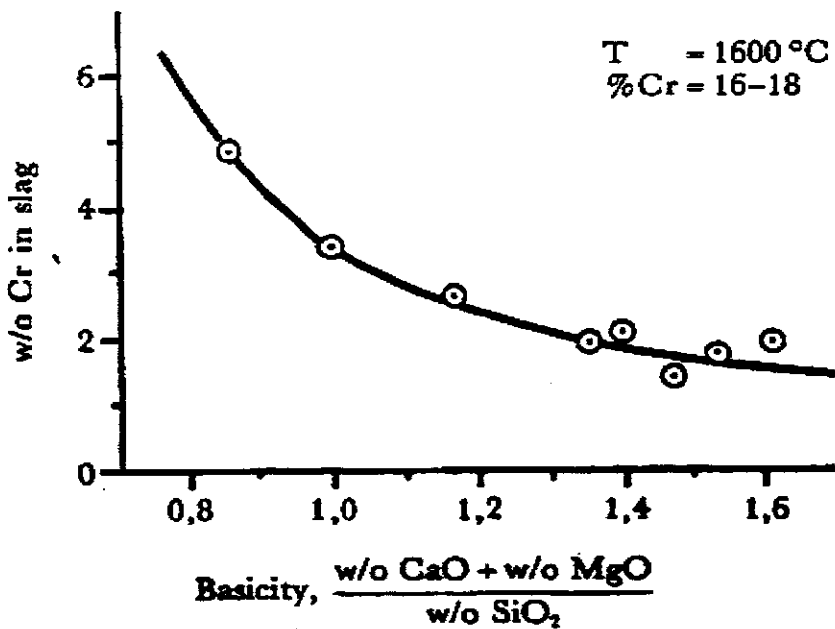


Figure 2. 1: Chromium content in slag as a function of the basicity in the system Ca-Mg-Fe-Cr-Si-O at $1600\text{ }^\circ\text{C}$ (Muan, 1984)

It can be seen from Figure 2.1 that controlling slag basicity is an effective way of reducing the loss of chromium to the slag, but the beneficial effect levels off significantly when the basicity exceeds a value of 1,6. The same effect has been reported by Holappa and Xiao, although according to these authors the effect levels off at basicity values higher than 1,4 as opposed to 1,6. However, the addition of lime to the slag to increase its basicity has a negative effect, in that it increases the slag volume and therefore the actual loss of chromium to the slag may increase even though the concentration of chromium in the slag decreases. Thus, in practical operations it is important to control the slag volume while decreasing the chromium oxides concentration in slags.

The addition of MgO into the slag has been reported to greatly improve the recovery of chromium with a basicity ratio of higher than 0,8 (Hollapa and Xiao, 2004). The presence of Al_2O_3 in the slag also enhances the chromium recovery. Experiments done by (Jansson A., Brabie, Fabo and Jansson S., 2002) indicated that the reduction rate of chromite ore decreases as the $\text{MgO}/\text{Al}_2\text{O}_3$ ratio in the slag increases. They concluded that, the gradual decrease of the reduction rate during the reduction reaction may be caused by the increase of the alumina and magnesia contents in slag that increases slag viscosity (the effect of viscosity during smelting and tapping processes is discussed in section 2.1.2). According to Riekkola-Vanhanen, 1999, the ratio between magnesium oxide and aluminium oxide influences the temperature in the furnace, and also the carbon content of the metal.

2.1.2. Slag viscosity

The viscosity of the liquid may be described as the measure of the resistance to flow of the liquid and the resistance to the movement of an object through the liquid. Thus, the viscosity is an important property that affects the separation of liquids. Liquids with a high viscosity are usually thick and flow slowly, while low viscosity liquids are generally thin and flow quickly.

Similarly, the viscosity of metallurgical slags plays a major role in clear separation of metal and slag, for example in the ferrochrome process, the higher the viscosity of the slag the more resistance it will have to the movement of the metal droplets through it, which would then result in ineffective separation. The effect of viscosity in the separation of two liquids may be explained by Stoke's law:

$$V_t = \frac{2gr^2(\rho_k - \rho_{liq})}{9\eta_{liq}} \quad (2.2)$$

Where, V_t is the terminal settling velocity of the falling object (a falling object in the case of a ferrochrome smelting process would be the metal droplets settling through the liquid slag), g is the gravitational constant, r is the radius of the metal droplets, ρ_k and ρ_{liq} are the densities of settling metal droplets and the liquid through which the droplets are settling (which is the slag) respectively, and η_{liq} is the viscosity of the slag. The time for the metal to settle due to gravity through the slag melt depends on slag depth (h) and the terminal velocity, and can be written as $t = h/V_{terminal}$, which leads the relationship:

$$V_{terminal} = \frac{h}{t} = \frac{2gr_{metal}^2(\rho_{metal} - \rho_{slag})}{9\eta_{slag}} \quad (2.3)$$

The rate at which the metal droplets are separated from the slag phase and settle at the bottom of the furnace is a function of the slag viscosity and in order to facilitate separation, viscosity needs to be as low as possible. This is shown in equation 2.3, where it is clear that the slag viscosity plays a significant role when it comes to the problem of metal entrainment in the slag, in that, if the slag viscosity is high, the settling time would be longer (compared to the tapping time), which would result in some metal droplets remaining entrained in the slag after completion of tapping. Also, high slag viscosity would decrease the terminal velocity of the settling metal which would also increase the chances of entrainment occurrence.

The viscosity also plays a major role in deciding the degree of completeness of reduction reaction, where low slag viscosity enhances rapid mass transfer, and thus, speeding up the whole process.

The viscosity of ferrochromium slags is strongly dependent on the composition of the slag (refer to the preceding section) as well as on the operating temperature. Close control of the slag composition is therefore essential for effective operation of the furnace. Figure 2.2 shows how the viscosity of the system MgO-Al₂O₃-SiO₂ changes with the additions of Chromium oxide, Iron oxide and Calcium oxide at different temperatures.

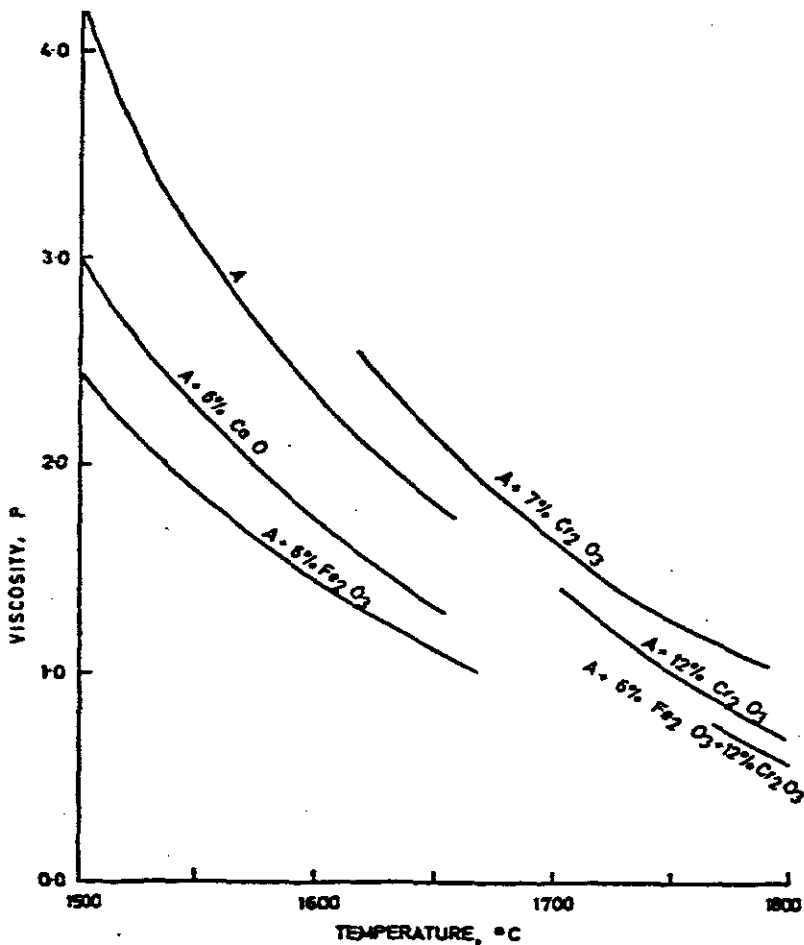


Figure 2. 2: Change in viscosity of slags after additions of CaO , Fe_2O_3 and Cr_2O_3 (Rennie, Howat and Jochens, 1972).

2.1.3. Liquidus temperature

The liquidus temperature of the slag is important as it determines the point of incipient crystallization, and significant increase in melt viscosity. The charge reacts and is heated as it descends towards the hot zone of the furnace, and it is not practically possible for the temperature of the alloy to be raised by an increase in its retention time in the furnace because, once the charge has reached the smelting zone and has fused, it will drop away from the area of intense heat surrounding the arcs and will settle to the bottom of the furnace. Consequently, for the alloy to be superheated to the required degree, the liquidus temperature of the slag must be sufficiently high to ensure that the slag is only sufficiently fluid for the products of smelting to drain away from the arc zone once the alloy has been heated to above its liquidus temperature.

Liquidus temperature is strongly influenced by the composition of the slag. This is clear from the following phase diagram (Figure 2.3):

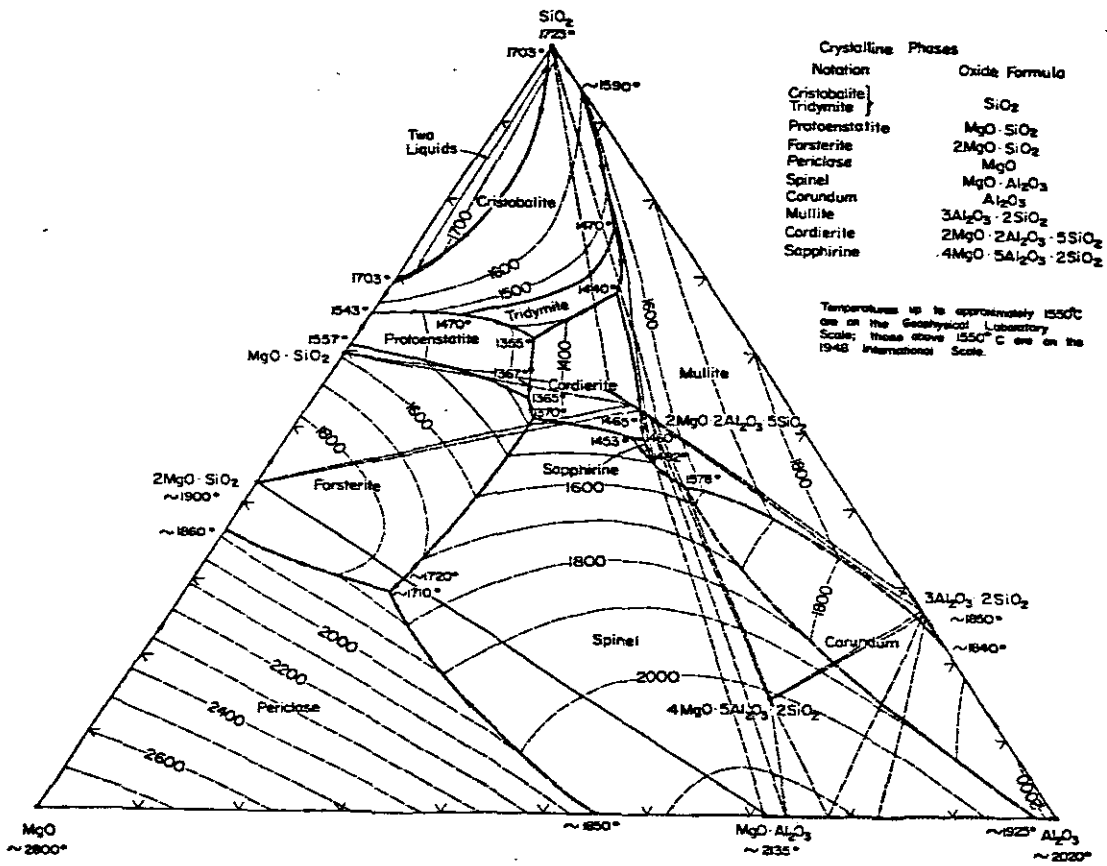


Figure 2. 3: System MgO-Al₂O₃-SiO₂; composite

A small change in composition, say from 70% MgO to 80% MgO leads to a dramatic rise in liquidus temperature, or alternatively, a significant spinel precipitation at constant operating temperature.

2.1.4. Density

Density is an intrinsic characteristic of a material, depending on its chemical nature and crystalline structure. It corresponds to the exact volume occupied by the material, without porosity and is thus a fundamental parameter contributing to the characterization of a product. Density measurement can be considered as a tool to follow the synthesis of a chemical substance or the sequence of a process, for example a smelting process. This is an essential characteristic in the study of ferrochrome slags as the knowledge of the density of slag produced would give an indication of the ferrochrome alloy losses to the slag product. The information can then be related to the smelter operating conditions and used to improve process control of the metallurgical processing plant.

The following equation can be used to determine the amount of ferrochrome lost as entrained alloy in slag:

$$x = \frac{\rho_m (\rho_s - \rho_{cs})}{\rho_{cs} (\rho_s - \rho_m)} \quad (2.4)$$

Where, x is the weight fraction of the entrained alloy in slag, ρ_m is the density of alloy produced, ρ_s is the density of a non-alloy slag and ρ_{cs} is the density of composite slag (slag produced as tapped from the furnace). The densities of the furnace products (alloy and slag) can be measured (or calculated), while the density of the non-alloy slag can be estimated using models based on partial molar volumes and mole fractions (discussed in 2.1.4.1).

True density of the material is calculated from the molecular weight and the crystalline lattice of the product which is determined by X-ray diffraction but this procedure is not common for such a determination, as diffractometry is not a routine technique (Viana, Jouannin, Pontier and Chulia, 2002). The instrument considered to give the closest approximation to the true density is the helium pycnometer, since helium penetrates into smallest pores and crevices and permits to approach the real volume of the material. The helium pycnometer offers the advantage of being easy to use and rapid which makes it suitable for routine analysis.

2.1.4.1. Model(s) for estimating the density of slags

An additive method for the estimation of densities in alloys and slags has been widely used; in which the molar volume, V , can be obtained from equations (2.5) and (2.6) below. M , x and \bar{V} are the molecular weight, mole fraction and the partial molar volume respectively, and the subscripts 1, 2 and 3 denote the various oxide constituents of the slag.

$$V = \frac{M_1 x_1 + M_2 x_2 + M_3 x_3 + \dots}{\rho} \quad (2.5)$$

$$V = x_1 \bar{V}_1 + x_2 \bar{V}_2 + x_3 \bar{V}_3 \quad (2.6)$$

The partial molar volume is usually assumed to be equal to the molar volume of the pure component but for slags containing SiO_2 and Al_2O_3 , densities estimated using this assumption are subject to error. This is because these slags consist of chains, rings and complexes which are dependent upon the amount and nature of the cations present. It is therefore necessary to make the partial molar volumes dependent upon composition for oxides of this type. Table 2.1 gives the recommended values of partial molar volumes for various oxides at 1500 °C.

Table 2. 1: Recommended values for partial molar volume \bar{V} of various slag constituents at 1500 °C (Keene and Mills, 1995)

Constituent	$\bar{V}/\text{cm}^3 \text{ mol}^{-1}$
Al_2O_3	$[28.31 + 32x_{\text{Al}_2\text{O}_3} - 31.45 x_{\text{Al}_2\text{O}_3}^2]$
CaF_2	31.3
CaO	20.7
FeO	15.8
Fe_2O_3	38.4
K_2O	51.8
MgO	16.1
MnO	15.6
Na_2O	33.0
P_2O_5	65.7
SiO_2	$[19.55 + 7.966x_{\text{SiO}_2}]$
TiO_2	24.0

2.1.5. Mineralogy

The behaviour of engineering materials such as slags; is typically derived from the chemical composition, mineralogical composition (or structure) and prior processing. Mineralogical analysis of the smelter products, in particular slags, is of utmost importance as it elucidates the reduction mechanism taking place in the furnace and based on that, alterations can be made to improve the process if required. However, limited efforts have been made towards understanding the mineralogy of ferrochrome slags.

According to Hayes (2004), the slag produced following the ferrochromium smelting contains significant quantities of chromium in the form of partially altered chromite (PAC) and entrained alloy. He further says that the PAC may contain a dispersion of fine iron or/and chromium metal alloy particles. A micrograph showing PAC in slag is shown in Figure 2.4.

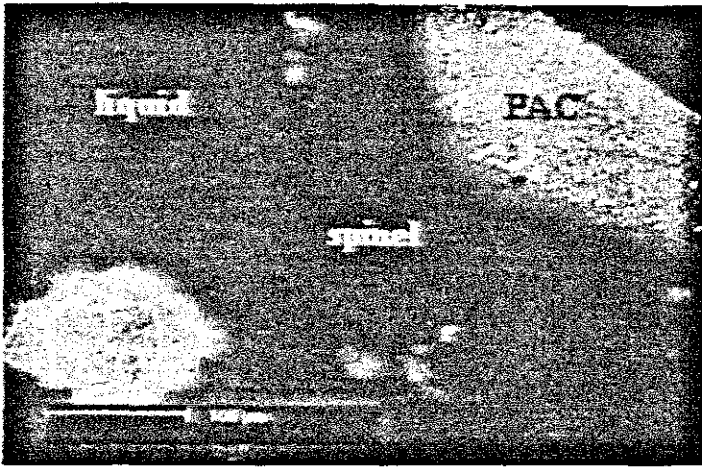


Figure 2. 4: Ferrochrome smelting slag at 1600 °C containing non-dissolved PAC (Hayes, 2004)

The addition of silica and the resulting formation of liquid slag can dissolve these partially altered chromites (PACs) and enhance the rate of reduction of chromium from the ore.

The existence of the PAC particles in the ferrochrome slag is also reported by Wedepohl (1984), although his mineralogical investigation was based on slag resulting from the treatment of South African chromite fines in a transferred-arc plasma furnace, in contrast to a submerged arc furnace.

Also present in the ferrochromium slag is the spinel $MgO \cdot Al_2O_3$ which is as a result of saturation occurring in the coke bed. The cooling of slag that is saturated with spinel leads to further precipitation on the existing solid surfaces of the PACs and therefore the formation of secondary spinels. The micrograph of the tapped slag in Figure 2.5 shows the formation of these secondary spinels.

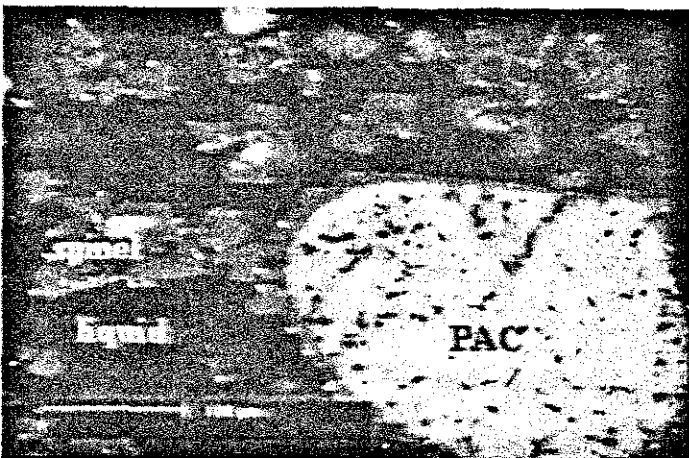


Figure 2. 5: Ferrochrome smelting slag “slow cooled” from the furnace showing the precipitation of secondary spinel (Hayes, 2004).

In general, the mineralogy of the slag is simple because only a few minerals are present; each mineral, however, shows chemical variability due to heterogeneity of the slag and differences in cooling rates. However, the mineralogy of ferrochrome smelter slag is complex due to the presence of chromium in a range of oxidation states.

2.2. Chemical analysis

There are various analytical techniques available for the determination of chemical composition. These include Inductively Coupled Plasma spectroscopy (ICP), X-ray Fluorescence Spectrometry (XRF), Atomic Absorption (AA) and many more, all of which have their advantages and disadvantages which must be considered when deciding on the technique to be used. Depending on the user's specific requirements and the nature of the samples to be analyzed, the considerations would be based mostly on sample preparation (i.e. ease and rapidity-turnaround time) and the level of accuracy of the method. The ICP and XRF are the most commonly used techniques in many industries including the ferroalloy producers. The technique in use at Ferrometals is the ICP, and only ICP and XRF are discussed in this section with XRF being the technique under investigation as a potential alternative technique to ICP.

2.2.1. Sampling and sample preparation

Sampling and sample preparation are the most important stages to the performance of any analytical process, whether the latter is laboratory based or process based. At Ferrometals, three samples of both slag and alloy are taken on a shift at an approximately three hour tapping interval. These samples are then submitted to the plant laboratory for analysis.

A typical processing of a slag sample once it is submitted at the plant (Ferrometals) laboratory is shown in Figure 2.6, each stage associated to potential sources of error. Here, a slag sample is crushed, divided (sub-sampling) in a stationary riffle into two equal samples, and one of the samples is homogenized by pulverizing in a swing mill (the other one is discarded). A laboratory sample of about 200g, representing the bulk sample, is then drawn from the homogenized sample (after mixing the sample by paper rolling) and, because this sample is not an immediate fit for analysis by analysis technique (ICP), a 0.2g test portion is drawn (by dipping) from it.

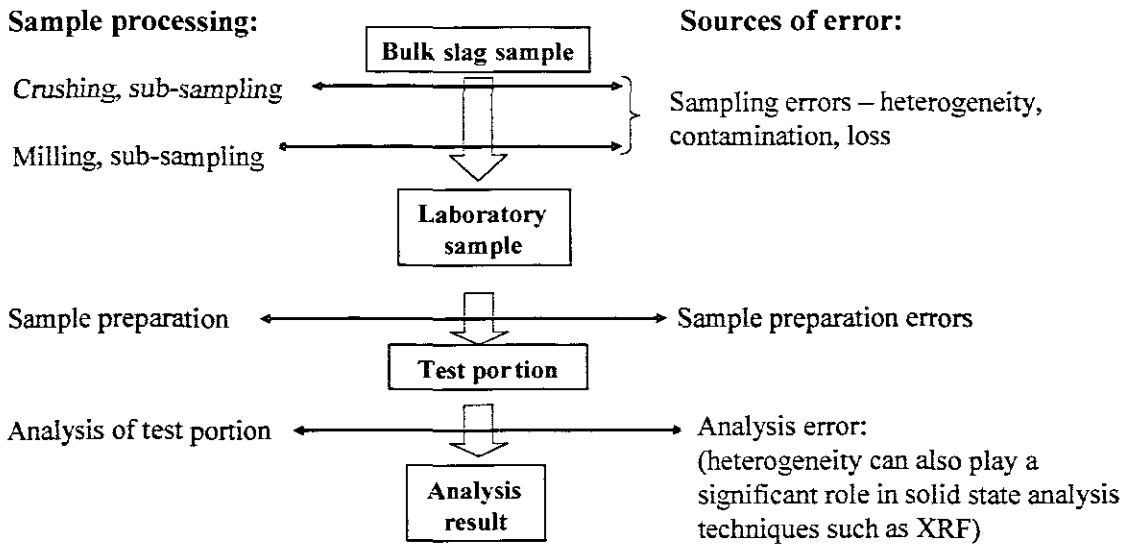


Figure 2. 6: Typical slag processing at laboratory

Depending on the analytical technique, the preparation of the test portion may be sample dissolution, fusion or pressing into a pellet (see sections, 2.2.2 and 2.2.3.1). At Ferrometals laboratory, this test portion is dissolved (the dissolution procedure is discussed in 2.2.2).

The total variance of an analytical determination is the sum of the variances of all individual sources of error shown in Figure 2.6, and thus, it is vital that all these aspects be considered carefully. Moreover, the precision in metal accounting can be written as (assuming that the variances are statistically independent):

$$V_{TMA} = V_M + V_S + V_{SP} + V_A \quad (2.7)$$

Where,

- V_{TMA} = the total metal accounting variance
- V_M = variance due to mass measurement
- V_S = variance due to all the sampling stages
- V_{SP} = variance due to sample preparation
- V_A = variance due to analysis

And thus, to achieve good metal accounting practices much effort must be put to minimizing these variances.

2.2.1.1. Sampling error(s)

Sampling errors arise both in the taking of the original sample and in attempting to take for analysis a small representative sample (sub-sampling) from a larger sample. Ferrochromium slags are not homogeneous (they are heterogeneous); they may have metal or alloy inclusions, and thus, sampling error(s) may exist throughout the sample processing (Figure 2.6). Gy (1982) refers to this type of sampling error(s) which is due to heterogeneity as the fundamental sampling error and its variance is called the fundamental variance.

The question of heterogeneity is strongly related to the concept of representativeness. If, for example, a sample is completely homogeneous, then any sub-sample selected would be perfectly representative of the sample regardless of the sampling strategy, but if the sample is heterogeneous, then it becomes difficult to select a representative sub-sample. Because of the heterogeneous nature of the slag, there is therefore an uncertainty as to whether the properties of the final test portion obtained through sample processing stages (Figure 2.6) are representative of the properties of interest of the bulk slag.

While other sources of error such as a biased selection of particles and analytical error can be minimized by the choice of sampling equipment, sample preparation and analytical technique, the fundamental error can only be reduced by increasing the sample size, where it is often assumed that the *fundamental variance* is inversely proportional to the sample mass (Geelhoed, 2005). How large the sample needs to be, depends on how large the relative variance of the fundamental error is compared to the maximum allowed error for a specific purpose. The subject of heterogeneity and the fundamental variance is clearly described by Gy's sampling theory which is dealt with in section 2.4.

Other sampling errors are due to human intervention, for example, at the plant laboratory after the sample has been crushed, any visible metal or raw material entrapped in the slag are removed by hand before the sample is homogenized, in which case the sample is definitely not representative.

2.2.1.2. Sample preparation errors

These are errors that occur during *sample reduction*, *sample mixing* and *sample division*. In selecting a method of sampling, the accuracy of the sample to be obtained is not the only

factor to be considered, but the ease or rapidity with which the sampling can be done, minimization of dust and avoidance of contamination are also of much greater importance.

Crushing and grinding (milling, pulverizing) can be major sources of contamination, resulting from abrasion of the crushing or grinding equipment, so efforts must be made to select the best possible equipment for each particular analytical task. Double jaw crushers are the best possible to be used as they can achieve a size reduction ratio of 25 (i.e. reduction from 50mm to 2mm in a single pass). Grinding is normally done in swing mills and careful choice must be made for suitable grinding vessels. Below is the list of various grinding vessels with possible contamination associated with each:

- Steel (Fe, Mn, Cr, Ni, Mo contamination)
- Carbon Steel (Fe contamination)
- Tungsten Carbide (W and Co contamination)
- Agate (Si and O contamination)
- Zirconia Ceramic (Zr and Hf contamination)
- Alumina (Al and Ga contamination)

Thus, the grinding vessel should be chosen such that the contaminants are not the elements of interest (i.e. a steel vessel cannot be used for grinding ferrochrome because of Fe and Cr contaminants).

One should mention the problem of malleable / ductile materials such as alloys compared to brittle materials such as clean slags, ceramics and refractories. Ductile materials become extruded, plate-like etc. Pulverization of a non-homogenous sample containing both ductile and brittle materials will therefore never lead to satisfactory size reduction of the ductile material.

Accurate division (sub-sampling) of powders and granular material into truly representative sub-samples is difficult and significant errors can be introduced in the process. Sub-sampling methods are well discussed by Gerlach and Nocerino (2003), and can be found in appendix C. These include sectorial splitter, incremental sampling, riffle splitting, alternate shoveling, coning and quartering, fractional shoveling, degenerate fractional shoveling, table sampler, v-blender, vibratory spatula, grab sampling.

2.2.2. ICP analysis at Ferrometals

The ICP analysis technique at Ferrometals is used to analyze the raw materials including reductants, as well as alloy and slag products. The technique involves dissolving the powder sample of 0.2g, obtained as explained in section 2.2.1, and analyzing the resulting solution. The dissolution procedure involves mixing the sample with Sodium Carbonate and Sodium Peroxide, and then fusing the mixture in a Zirconia crucible. The fused mixture is then dissolved in Nitric acid before the appropriate standards for the ICP are added, and the solution made up to volume by adding distilled water.

The whole process of dissolving the samples takes about 50 minutes per sample and with all the other samples (including raw materials and alloy) that need to be analyzed, slow turnaround times are evident. As a result not all three slag samples (and alloy) tapped on a shift were analyzed, but only one sample of each product (i.e. slag and alloy) from the first tapping (this was the case during the initial investigations and has improved since the start of this project).

The slag composition in conjunction with tapping temperature has been shown to have significant impact on the efficiency of a smelting process (see section 2.1.1.), and thus, is an important property that can be (or is) used by the metallurgists to identify and rectify deviations in the process for improved efficiency. Thus, maintaining efficient process performance would be possible if all the samples taken on a shift are analyzed. This would mean that a slag sample taken during each tapping process should immediately be submitted to the laboratory, and its analysis results should be available before the next tapping rather than having the analysis results before the next shift.

Regarding the reliability of the analysis results, it can be said that the analysis procedure itself including the dissolution stage is correct as the appropriate solution and calibration standards are used. However, as mentioned in section 2.2.1.1, the removal of the entrapped material during sample preparation leads to biased samples, which in turn leads to incorrect mass balances. This implies that as much as the analysis results are correct, they cannot be trustworthy if the analyzed sample itself has already been biased. Moreover, a small analysis sample of 0.2g could result in severe biases due to non-representativity of samples, for example, in a situation where there could be particles of ferrochrome in the slag.

Given the above mentioned facts it would be worthwhile therefore to investigate an alternative analysis technique that would allow rapid sample preparation method in contrast to the dissolution for ICP and may be use a larger analysis sample rather than the 0.2g sample. Such a technique may be an XRF as this uses pulverized samples pressed into pellets and a sample as large as about 8g.

2.2.3. Theory of X-ray Fluorescence spectrometer (XRF)

Most of the work done on the XRF technique is based on the analysis of rocks and geological samples (6, 14, 22, 26, 34), and therefore not much literature has been found which deals specifically with the analysis of either chromite or ferrochromium samples. The discussion which follows is a general overview of the sample preparation, calibration and analysis methods involved.

2.2.3.1. Sample preparation techniques

The sampling and sample preparation stages discussed in section 2.2.1 (Figure 2.6) also apply in the preparation process for XRF analysis; the exception is the preparation of the test portion for which dissolution was the method used for ICP. For XRF analysis, two techniques for preparing samples are largely used and they are fused glass beads (FGB) and pressed powder pellets (PPP) and; throughout the discussion these will be referred to as specimens. The requirements for an adequately prepared specimen whether a FGB or a PPP are that it should:

- Be representative of the material
- Be homogeneous
- Have a flat, smooth and reproducible surface
- Be thick enough to meet the requirements of an infinitely thick specimen

The choice between the two specimens is made based on accuracy required, variation of sample matrix, concentration levels and turn around time. The PPP is easy and fast to prepare but has disadvantages of introducing particle size effects, mineralogical effects, and surface roughness (can be avoided by using suitable sample preparation techniques, e.g. fine grinding). The preparation of FGB on the other hand is time consuming but particle size and mineralogical effects can be minimised. This is because fusion (if complete) destroys the mineral grains and their structures, thus distributing constituent elements homogeneously

throughout the mass and eliminating the grain size effect and mineralogical effect on mass absorption (La Tour, 1989).

FGB preparation

The technique consists of dissolving the powdered sample in a solvent called a flux at high temperature ($>1000\text{ }^{\circ}\text{C}$) in a suitable (platinum / gold) crucible and casting it in a casting dish. The most current used fluxes are borate such as sodium tetraborate, lithium tetraborate, lithium metaborate or sometimes polymetaphosphates. The result of the fusion is the production of a homogeneous glass bead. Most mixtures also include other compounds to act as a heavy absorber to further reduce mass absorption effects, oxidiser to prevent alloying with the crucibles, and compounds that reduce surface tension of the melt (Qiao and Xiaomin, 2002).

Fusion of materials such as chromite and ferrochrome into a glass has been reported (Sear, 1997 and [1]) to be difficult in that these materials tend to attach on platinum crucibles; as a result high dilutions have to be made which lead to poor sensitivity for minority elements. Solutions to this problem such as the use of other crucibles (alumina), and the addition of sintering / oxidation stage before fusion with flux have been reported. However, they require more effort and would lead to even slower turnaround times than dissolution procedures for ICP.

PPP preparation

A powder with or without a binder, is poured into a die and compressed in a hydraulic press for a given time at a given pressure. Pressure plays an important role in that, according to (author ref 6), when too low pressure is applied in combination with too little time an inconsistent pellet would result and, too high pressure applied would cause cracking in the pellet. A general guideline is that, if the particle size of a sample is $\leq 85\text{ }\mu\text{m}$, it will form a pellet at a pressure of 5 tons/in^2 .

The preparation of pellets is easier when binders are used as they produce solidity to the pellets; few effective binders include graphite, chromatographic-grade cellulose, ethyl and methyl cellulose, polyvinyl alcohol (i.e. Mowiol in aqueous solution), starch etc. (Tertian and Claisse, 1982). Binders must be completely free of analyte or interfering elements; they must

be stable in air, vacuum and under X-ray excitation; and they should have minimal absorption of the analyte elements.

It has been mentioned by few authors (La Tour, 1997. Mori, Reeves, Correia and Haukka, 1999) that the pressed powder pellets are not suitable for analysis of light elements such as Si, Al, Na, Mg due to mineralogical effects.

However, Qiao and Xiaomin (2002) have analysed chromite samples by pressed powder pellet technique and their results compared well with the wet chemical analysis within the acceptable precision.

2.2.3.2. Calibration and matrix effects

Calibration is necessary in any analytical technique in order to obtain good results. In quantitative XRF analysis, the calibration procedure, with the aid of reference materials or standards transforms the measured X-ray fluorescence intensity of a particular analyte to concentration. At least 15 standards are required to cover the expected concentration range of the samples, and these should be chemically similar to the samples. In addition, for PPP technique, the standard should be a matrix compositionally similar to the samples. The general calibration equation relating concentration and the net peak can be written as:

$$C_i = D_i + E_i R_i M \quad (2.8)$$

Where, R_i is the intensity of element i in kilocounts per second (kcps), E_i is the slope of the calibration curve for element i , D_i is the intercept of the calibration curve for element i and M is the matrix correction coefficient.

Matrix effects result from the fluorescence radiation being absorbed by coexisting elements, causing reduced intensity, or enhancement of radiation due to secondary radiation from coexisting elements, causing increased intensity. The major causes of matrix effects are variations in absorption, enhancement, particle size and surface effects, and effects due to chemical state. Figure 2.7 shows an example of the effect of enhancement on the calibration curve for Cr in a FeCr alloy sample. In this figure, Fe enhances Cr, causing the calibration line to lie above the straight line expected from a pure element calibration.

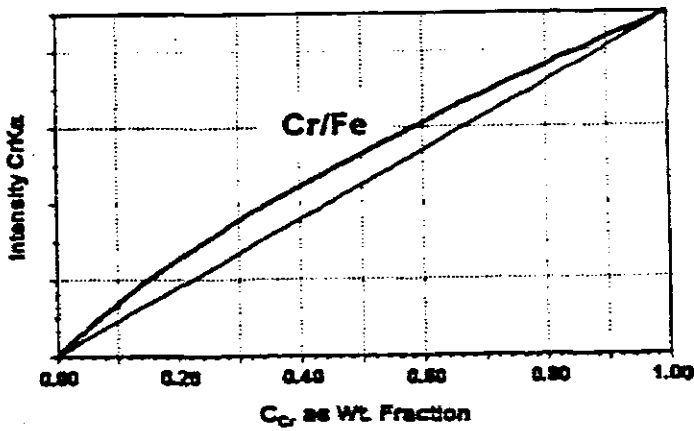


Figure 2. 7: Calibration curve for Cr in a FeCr alloy (Willis, 2004)

To obtain a straight calibration line, the effects have to be corrected for by including the matrix correction term, M_i , in the calibration equation (see equation 2.8). Many different models are available for the calculation of the matrix correction coefficient (Willis, 2004), and are readily installed in the spectrometer software. Thus, they are calculated automatically by the software. Figure 2.8 shows examples of two calibration plots, one with matrix correction and the other one with no matrix correction done.

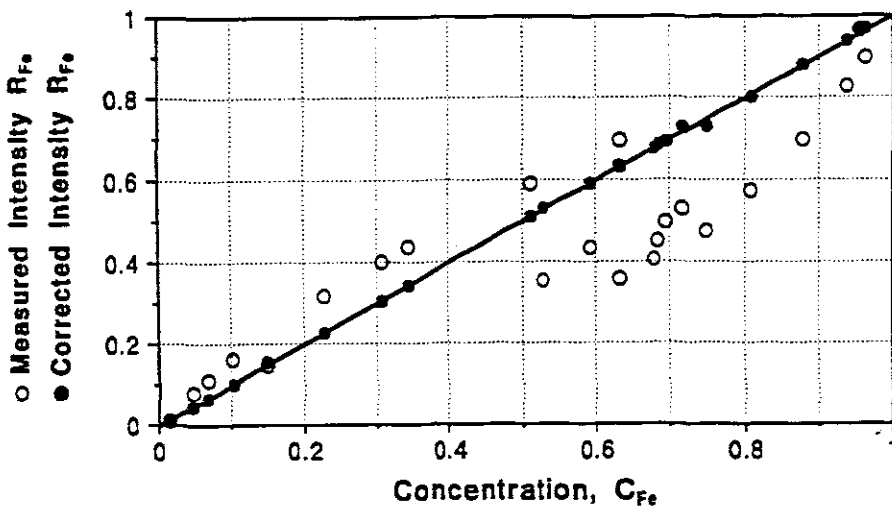


Figure 2. 8: Calibration plots for Fe in stainless steel (Willis, 2004)

It is important to note that proper sample preparation, be it fused bead or powder pellet plays a crucial role in obtaining a reliable calibration line, as no amount of correction can improve the quality of the analytical result if the sample is poorly prepared.

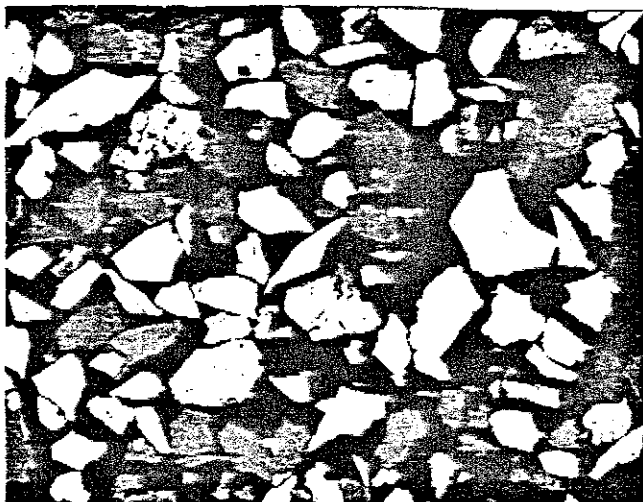


Figure 2. 9: Example of a BSE image

The BSE image is the most informative image for mineralogical applications because it shows the distributions of minerals and can provide qualitative information on trace elements in the minerals. Furthermore, when using polished surfaces, the image is free of the effects of topography, fine scratches generally do not appear in the image and holes in polished sections are readily detected.

The SE detector displays the SE signal as a grayscale SE image. The image shows the distribution of minerals and some topographic effects because the SE signal is based on a combination of the average atomic number of the mineral and the topography of the sample. Thus, the SE image is not as useful as the BSE image for showing mineral distributions, but it displays details of surface irregularities.

The main advantage of SEM is that many minerals can be discriminated from each other in produced BSE images, in contrast to the relatively few minerals that can be discriminated in images produced with an optical microscope. The minimum size of the particle that can be detected and identified is dependent on the magnification. Particles greater than 1 μ m can be detected, identified and segmented from images produced at a magnification of 400X.

2.4. Heterogeneity

When a sample is selected from the bulk material whether for chemical analysis or physical measurement, it should be representative of the bulk. The reason that samples do not exactly mimic the bulk materials that they are supposed to represent is because of the sampling errors associated with heterogeneity. These errors contribute to the uncertainty in the analysis results for the assessment of the quality of a product or the feasibility of a process.

Heterogeneity is a condition of the bulk material (or sample) when all the individual particles are not identical with respect to the characteristic of interest, for example, differences in particle size, density and chemical composition. The differences in the chemical and physical properties of the material result in what is referred by Gy as the *constitutional heterogeneity* or *intrinsic heterogeneity* (Pitard, 1993), which is the focus of this section. It has been shown in chapter 1 that the ferrochromium slag has alloy entrained in it, and thus, differences in density are evident and are presumed to result in constitutional heterogeneity nature of the slag.

The existence of this type of heterogeneity leads to an unavoidable sampling error called the fundamental error. The variance of the fundamental error (fundamental variance) represents the smallest sampling variance that can be achieved without altering individual particles and exists even when the sampling procedure is correct.

As mentioned in the section 2.2.1.1, the fundamental sampling error can only be reduced by increasing the sample mass and this can be done if a value for its variance is known. Gy (1982) has developed a theory of particulate sampling for applications in the mining industry, which enables the estimation of the fundamental variance. Its applications are discussed by few authors including Pitard (1993), Assibey-Bonsu (1996) Geelhoed (2005), François-Bangarçon, Gerlach and Nocerino (2003). Lyman (1986, 1998) has introduced a new approach to the theory and demonstrated its application to the sampling of coal.

2.4.1. Estimation of the relative variance of the fundamental error, σ^2

In order to understand the following discussion, it is important to define some basic concepts of Gy's theory as these will be used throughout. In Gy's theory, the chemical or physical component whose proportion in a sample (lot) is of interest is called the *critical component* and its proportion by mass in a lot, sample or particle is called the *critical content*. The word

'lot' refers to the bulk sample (in cases of products from smelter operations such as solid slags) or the collection of particles from which a portion is to be taken, and the *sample* is the portion taken to represent the lot.

The relative variance of the fundamental error is related to several properties of a sample (Gy, 1982), by the general formula:

$$\sigma^2 = c f g l d^3 \left(\frac{1}{M_s} - \frac{1}{M_L} \right) \quad (2.9)$$

Where σ^2 , M_s and M_L are the sampling relative variance, the mass of the sample (g) and the mass of the lot (g) respectively, c is the mineralogical factor, l is the dimensionless liberation factor, f is the dimensionless particle shape factor, g is the dimensionless particle size range (or granulometric) factor, d is the nominal size of the particles.

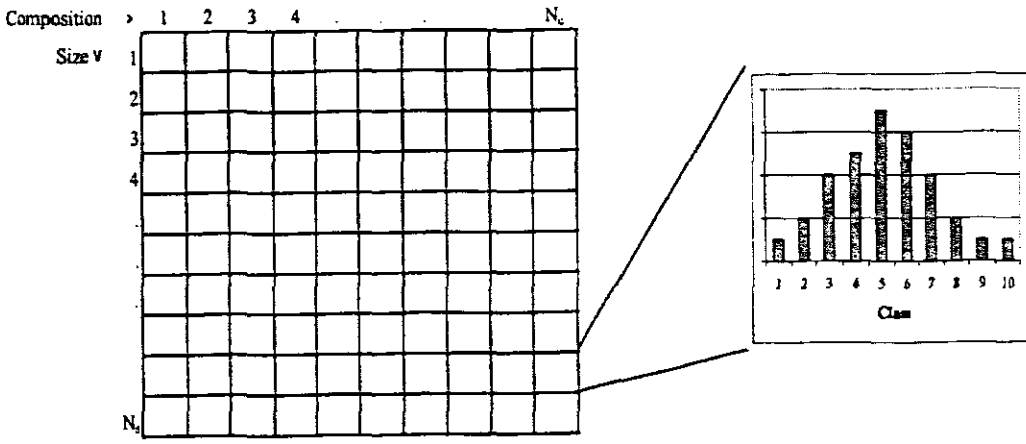
Since c , f , l and g are constant for a particular material; their product can be written as one sampling constant K_s (g/cm^3), and when the sample is much smaller compared to the lot (i.e. $M_s \ll M_L$), then the term $1/M_L$ is negligible and equation 2.9 takes the simplified form:

$$\sigma^2 = \frac{K_s d^3}{M_s} \quad (2.10)$$

The difficulty of estimating the liberation factor has been reported (Carrasco, 2005, François-Bangarçon, Gy, 1982), although some models have been proposed their applications have limitations. Thus, it is difficult (even impossible for most materials) to estimate the K_s value in equation 2.10.

Lyman (1986, 1998) has derived a rather simpler expression for the estimation of the sampling constant (K_s), using Gy's definition of constitutional heterogeneity.

To understand the concept of constitutional heterogeneity or sampling theory, visualize that the material is separated into various size fractions by sieving or some other suitable method. Then, for each size fraction, imagine that the particles are all sorted into composition classes. This is illustrated in the diagram below.



Gy's definition of constitutional heterogeneity is then given as:

$$CH_L = \frac{N_F}{M_L^2} \sum_{i=1}^{N_F} \frac{(a_i - a_L)^2 M_i^2}{a_L^2} \quad (2.11)$$

where, CH_L is the constitutional heterogeneity, N_F number of particles in the lot L, M_L is the mass of the lot, a_i is the critical content or composition of the particles within the i^{th} particle class, a_L is the critical content of the lot and M_i is the mass of the material in the i^{th} particle class.

According to Lyman (1998), the definition (equation 2.11) can be written in terms of sums over size and density classes for particles in the nominal or expected make-up of the material. Thus, M_i can be replaced by $m_{uv} = V_u \rho_v$ and the number of particles in a particle class within the lot of mass M_L can be taken to be n_{uv} resulting to the expression:

$$CH_L = \frac{N_F}{M_L^2} \sum_{u=1}^{N_u} \sum_{v=1}^{N_v} \frac{(a_{uv} - a_L)^2 n_{uv} m_{uv}^2}{a_L^2} \quad (2.12)$$

Taking X_u to be the mass fraction of particles in the u^{th} size fraction and Y_{uv} to be the mass fraction of particles in the v^{th} composition class within the u^{th} size class leads to the expression:

$$CH_L = \frac{N_F}{M_L} \sum_{u=1}^{N_s} X_u V_u \sum_{v=1}^{N_d} \rho_{uv} Y_{uv} \frac{(a_{uv} - a_L)^2}{a_L^2} \quad (2.13)$$

M_L/N_F is the average fragment mass in the lot so that CH_L is effectively a constant for the material and is not a function of the quantity of the material in consideration (Lyman, 1998). The quantity $CH_L M_L/N_F$ can be taken to be the *sampling constant*, K_s , for the material, and thus, equation 2.13 becomes:

$$K_s = \sum_{u=1}^{N_s} X_u V_u \sum_{v=1}^{N_d} \rho_{uv} Y_{uv} \frac{(a_{uv} - a_L)^2}{a_L^2} \quad (2.14)$$

With the first and second expressions representing the heterogeneity based on size factors (CH_s) and density factors (CH_v) respectively.

Because of the density difference between the ferrochrome slag and the entrained alloy in it, it would be worthwhile to evaluate the application of equation 2.14 to this particular material, so as to be able to calculate the fundamental variance via equation 2.18. The *entrained alloy in slag* can be used as the *critical component* and its content can be determined by equation 2.4. Equation 2.14 then becomes:

$$K_s = \sum_{u=1}^{N_s} X_u V_u \sum_{v=1}^{N_d} \rho_{uv} Y_{uv} \frac{\left(\left(\frac{\rho_m (\rho_s - \rho_{cs})}{\rho_{cs} (\rho_s - \rho_m)} \right) \times 100 - a_L \right)^2}{a_L^2} \quad (2.15)$$

The only requirement for the application of the above described model is the knowledge of the size distributions of the critical component as well the density distributions of the material in the specific size fractions. The size distributions can be determined by either sieving or image analysis, depending on the particle sizes. A gravity separation technique (jig, shaking table, etc.) can be used for separating into density distributions and the densities measured by pycnometer.

The model also requires the knowledge of particle volume distributions which can be calculated using the equation (Hogg, 2003):

$$w_{ij} = \rho_{ij} \phi_{ij} x_j^3 \quad (2.16)$$

Where, w_{ij} is the mass of a single i -particle of size j , ρ_{ij} is the density, x_j is the particle size and ϕ_{ij} is the shape factor which depends not only on the shape of the particle, but also on the particular definition of size. For size measurements presented as “equivalent-sphere diameter”, it is reasonable to use the shape factor for a sphere, which is $\pi/6$. Substituting ρ_{ij} by w_{ij}/v_{ij} and rearranging results in the expression:

$$v_{ij} = \phi_{ij} x_j^3 \quad (2.17)$$

And, v_{ij} is the volume of a single i -particle of size j .

2.4.2. Sampling Constant – definition and use

Lyman defines the sampling constant as a quantitative measure of the material intrinsic heterogeneity with respect to a particular critical component (the component of the material to which heterogeneity evaluation is based), and has the basic formula given in equation 2.14. It captures all the necessary information about the heterogeneity of the material to be sampled and has the units of mass (i.e. if the particle volume is calculated in cm^3 , and the particle density has units of g/cm^3 , the sampling constant will have units of g).

It should be noted that the material can be very heterogeneous (i.e. has large sampling constant) with respect to one critical component and nearly homogeneous with respect to some other critical component. This implies that the sampling constant depends on all the individual components in the material and that a different value should be determined for individual components.

Knowledge of the sampling constant for a material permits the calculation of the expected variance (equation 2.18) between nominally identical sub-samples of a given mass. This means that if some mass of material is put through a rotary sample divider and nominally identical sub-samples of mass M_s are formed, the variance in the true analysis of the sub-samples with respect to a particular critical component cannot be less than the value calculated from the sampling constant. In practice, if the sub-samples were all prepared for

analysis with great care, the variance between the analyses from each sub-sample would be larger than the value calculated from the sampling because the analytical results would also involve a component of variance due to the uncertainties in the analytical procedure.

$$\sigma^2 = \frac{K_s}{M_s} \quad (2.18)$$

Alternatively, the sampling constant can be used to determine the sample mass that must be retained (taken / sampled) to ensure that the RSD between nominally identical samples does not exceed a fraction σ , then:

$$M_s = \frac{K_s}{\sigma^2} \quad (2.19)$$

For example, if $\sigma = 0.02$ (2% relative), then:

$$M_s = \frac{K_s}{0.0004} = 2500K_s$$

Equation 2.18 may also be rewritten as follows, to enable the calculation of the percent relative standard deviation (% RSD):

$$\%RSD = 100 \times \sqrt{\frac{K_s}{M_s}} \quad (2.20)$$

3. RESEARCH METHODOLOGY

The slag samples from Samancor Chrome's Ferrometal's plant in Witbank were used for the purpose of the investigation. The samples were tapped from furnaces, 3, 4 and 6, each sample weighing about 1 kg. This chapter details the sample preparation and analysis procedures followed, as well as the equipment used in the investigation, which are described under three sections. The sections include the determination of slag composition, the determination of the entrained alloy in slag and the characterization of heterogeneity. The following characterization techniques were utilized: X-ray Fluorescence (XRF) spectrometer for chemical characterization, Pycnometer for density measurements, Scanning Electron Microscopy interfaced with an energy dispersive X-ray analyzer (SEM/EDX) for size distributions and mineralogy; and lastly the shaking table for gravity (density) separation, combined with screening to determine the constitutional heterogeneity.

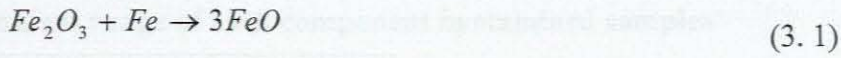
3.1. Slag chemical characterization

The slag samples were analyzed for six major elements (SiO_2 , CaO , Al_2O_3 , MgO , Cr_2O_3 , and FeO) on a Philips 1404 automatic Wavelength Dispersive XRF spectrometer, equipped with a Rhodium X-ray tube. The spectrometer can load a maximum of 72 samples at a time. The technique used was a powder pellet which required that the slag samples ground into powder and then pressed into pellets (the preparation is described in section 3.1.2). As for any analytical technique, the XRF spectrometer had to be calibrated before measurements of the slag samples were performed and a number of standards were required for this purpose. Thus, standard samples with similar composition to the slag samples under investigation were prepared for the spectrometer calibration. Section 3.1.1 describes how these standard samples were prepared and the calibration method is described in section 3.1.3.

3.1.1. Standards preparation

3.1.1.1. Reagents used

Analytical reagent-grade compounds of SiO_2 , CaO , Al_2O_3 , MgO , Cr_2O_3 , Fe_2O_3 and Fe metal were used to prepare the standard samples. However, Fe_2O_3 and Fe were used to prepare FeO in which stoichiometric proportions were mixed following the equation:



The mixture was pressed in a hydraulic press at about 12 KPa to form a pellet which was then sintered for 12 hours in a tube furnace set at 900 °C in argon atmosphere. The gas (Argon) was purified by passing through silica gel and MgClO_4 to remove moisture, and through a column of ascarite to remove CO_2 impurity. It was then passed through a column of Cu turnings at 500°C to remove the traces of oxygen impurity before being admitted into the furnace (schematic diagram of the setup is shown in Figure 3.1). The sintered pellet was then pulverized and stored under absolute alcohol to prevent re-oxidation of iron to ferric iron. This method for preparing FeO was adopted from Banda, 2001. The prepared FeO was used in standards preparation.

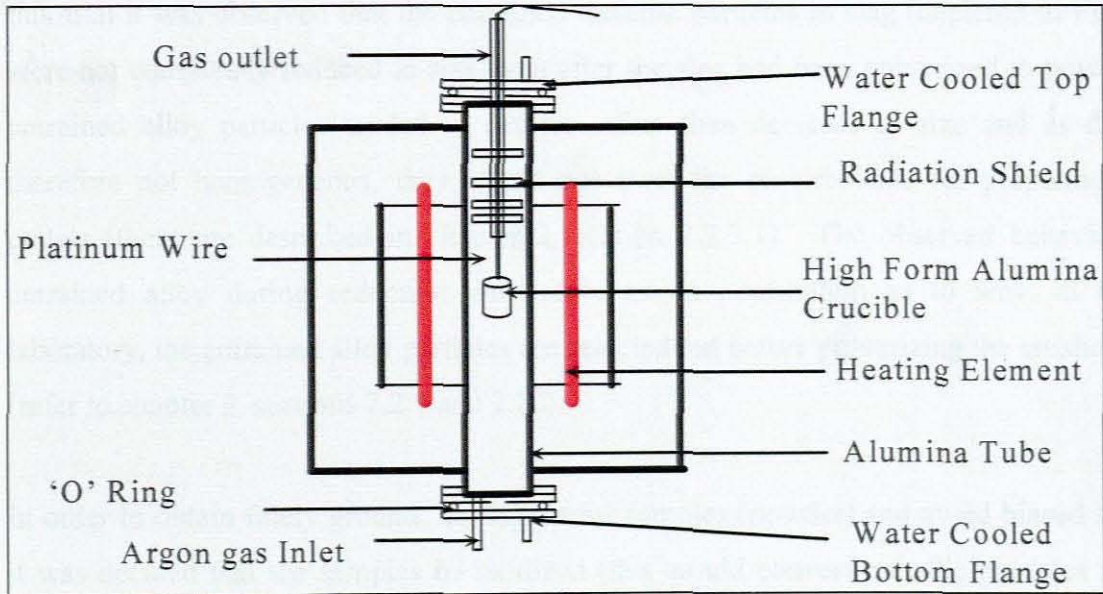


Figure 3. 1: Schematic diagram of the tube furnace set-up (Banda, 2001)

3.1.1.2. Method

About 200 g mixture of SiO_2 , CaO , Al_2O_3 and MgO was melted in an induction furnace using graphite crucibles, to form a master slag which was then cooled and pulverized. The pulverized slag was then heated for 8 hours in a muffle furnace at 700 °C, to burn off carbon contamination from the graphite crucibles. Different proportions of Cr_2O_3 and FeO were added to the master slag and the mixtures homogenized (in an agate mortar under acetone), to obtain various slag standards covering the range of the actual slag. The composition ranges covered by the standards, including the ones that were available is shown in Table 3.2.

Table 3. 1: Content range of each component in standard samples

Component	Range, wt%
Al ₂ O ₃	16 – 43
CaO	1 – 6
Cr ₂ O ₃	6 – 18
FeO	3 – 11
MgO	10 – 29
SiO ₂	13 – 39

3.1.2. Sample preparation

A trial sample preparation was done before deciding on the procedure to be followed. From this trial it was observed that the entrained metallic particles in slag (depicted in Figure 1.2) were not completely reduced in size even after the slag had been pulverized to powder. The entrained alloy particles tended to deform rather than decrease in size and as they were therefore not homogeneous, they would not meet the requirements for preparing powder pellets (these are described in chapter 2, section 2.2.3.1). The observed behavior of the entrained alloy during reduction may serve as an explanation as to why, at the plant laboratory, the entrained alloy particles are selected out before pulverizing the crushed sample (refer to chapter 2, sections 2.2.1 and 2.2.2).

In order to obtain finely ground, homogeneous samples (powder) and avoid biased sampling, it was decided that the samples be oxidized (this would convert metallic particles into their oxides), after the pulverizing stage. The following paragraphs describe the procedure followed.

Slag samples from furnaces, 3 and 6, were crushed individually with a jaw crusher and then a cone crusher to ± 10 mm. Each crushed product was split into two equal sub-samples using an open riffle. One of the sub-samples was pulverized in a swing mill and then oxidized by heating in a muffle furnace set at 900 °C, using boat alumina crucibles. During oxidation, the samples were left in the furnace overnight after which they were pulverized again, put back into the furnace for 3 to 4 hours and pulverized again.

The second sub-sample was prepared by mechanically selecting out 'visible' entrained alloy species before pulverizing in a swing mill. This is what is done at the plant laboratory and it was done in this study to compare the results with those obtained by the method described above.

Pressed powder pellets were then prepared from the powder samples (oxidized and non-oxidized), and the prepared standards. From each sample to be analyzed, about 8 grams of powder was taken and mixed with 1 ml of Mowiol solution which is a binder prepared by dissolving polyvinyl alcohol in water. The mixture was blended in an agate mortar using the agate pestle until the Mowiol solution was adsorbed into the powder and then dried in the oven at 60 °C for about 1 hour or until the sample was almost dry. The dried sample was then grounded, transferred into a stainless steel pill-maker (consisting of a cylinder, a base and a plunger), and compressed at a pressure of 10 tons for 1 minute using a hydraulic press. A prepared powder pellet is shown in Figure 3.2.

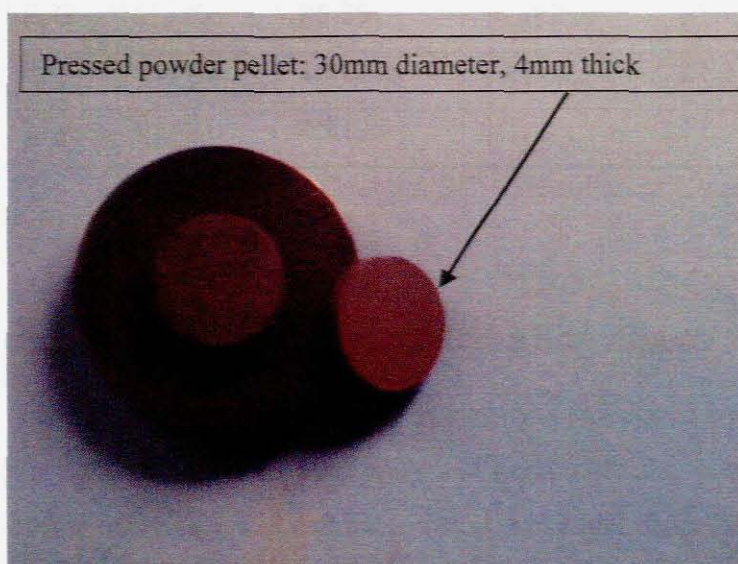


Figure 3. 2: Pressed powder pellet

3.1.3. Calibration and analytical conditions

The spectrometer was calibrated for the elements of interest (refer to Table 3.1) by analyzing ten powder pellets prepared from the standards. When calibrating, a least-squares regression analysis and statistical evaluation is carried out for each element by the spectrometer software (SuperQ), resulting regression equations of the form given in equation 2.8.

$$C_i = D_i + E_i R_i M \quad (2.8)$$

This equation is described in chapter 2, section 2.2.3.2. The matrix correction coefficients (M) were calculated automatically by the software.

The spectrometer X-ray tube was operated at 50 kV and 50 mA, with exception of Cr_2O_3 for which the tube operated at 60 kV and 40 mA. The analytical conditions are summarized in Table 3.2.

Table 3. 2: Analytical conditions

Element	Line	Angle 2θ , degrees	Analyzing crystal	Detector	Count time, seconds
Al_2O_3	$\text{K}\alpha$	145.01	PE	FL	20
CaO	$\text{K}\alpha$	113.23	LiF200	FL	20
Cr_2O_3	$\text{K}\alpha$	107.21	LiF220	FL	50
FeO	$\text{K}\alpha$	85.75	LiF220	FL+SC	50
SiO_2	$\text{K}\alpha$	109.185	PE	FL	20
MgO	$\text{K}\alpha$	45.125	TAP	FL	20

FL – Flow proportional Counter, SC – Scintillation Counter

3.2. Density and entrained alloy characterization

The amount of alloy entrained in slag was calculated by equation 2.4, described in chapter 2. The densities of both pure alloy and composite slag were measured by pycnometer, and that of non-alloy slag was estimated using the model described in section 2.3.1

The pycnometer used is a manual Micrometrics multivolume 1305. It can be operated with different sample cup sizes (5 cm^3 , 35 cm^3 and 150 cm^3), depending on the available quantity of the sample and can determine the density of both powders and solids. Measurements were performed using a 35 cm^3 sample cup in this study. The pycnometer uses helium or any other dry non-corrosive gas (in this work Nitrogen gas was used), to determine the volume of the sample, by measuring the pressure change of the gas in a calibrated volume. The sample volume is calculated based on this pressure change and then with the known weight of the sample, the density is then calculated.

3.3. Heterogeneity characterization

In order to characterize heterogeneity in the ‘tapped’ slag samples, the entrained alloy in slag was chosen as the critical component to which all the calculations were based. The choice was based on the principal requirement that the content of the chosen component in a sample can be measured (Hogg, 2003). Thus, the decision was based on the fact that the alloy content could be easily measured using the method described in section 3.2 above. Furthermore, the method used for estimating the variance (or relative error) due to constitutional heterogeneity as adopted from Lyman, 1998 requires the knowledge of the size distributions of the critical component. This was achieved by image analysis and is explained in section 3.3.1.

Density was chosen as the characteristic for evaluating heterogeneity as a density difference was expected between the entrained alloy and slag. Lyman’s method suggests that the material in each size fraction be separated into at least ten density increments. However, in his work he also demonstrated that the results from one top size fraction can be used as a basis for heterogeneity calculations. Therefore, only the material in the largest size fraction (based on entrained alloy size distribution) was separated into density fractions (section 3.3.2).

3.3.1. Estimation of size distributions

The size distributions of alloy entrained in slag were estimated by image analysis using SEM/EDX analyzer which required that samples be cut and polished. The slag samples used were tapped (or sampled) from five consecutive taps with two samples (i.e. sample 1 and sample 2) taken from each tap. A Leo 1430VP SEM fitted with Backscatter and Cathodoluminescence detectors was used.

3.3.1.1. Sample preparation

The samples were prepared by cutting thin pieces from each of the bulk samples with a diamond cutter and then mounting each piece into resin. Three pieces were cut at various sections of each sample (e.g. three pieces were cut from a sample of the fifth tap, mounted individually, and were named T₅A, T₅B and T₅C). The mounted pieces which will be referred to as specimens were then grounded with SiC paper of grit sizes 320 – 1200 and polished on special polishing cloths using 3 μ m and finally 1 μ m diamond suspensions. The polished

specimens were then coated with a thin layer of carbon to prevent charging on the sample, as the SEM produces an electron beam under high vacuum, before they were analyzed.

3.3.1.2. Size analysis

Backscattered electron (BSE) images of the prepared specimens were produced by using SEM at a magnification of 900X. Approximately four images were taken from each specimen, at various positions as it is not possible to take an image of the whole specimen at once. The sizes of the entrained alloy particles were then manually measured from the produced images in terms of sphere (or circle) diameters, using imaging system software. From this software it was possible to count the measured particles and classify them into various size classes.

3.3.2. Separation into density distributions

The size distribution analysis described in section 3.3.1 above revealed that the entrained alloy appears in very small sizes (micros) as it can be seen in the results section. Thus, to be able to liberate the alloy particles or at least bring them to near liberation, the slag samples had to be reduced in size. This was done by crushing them through jaw and cone crushers, and then ground in a rod mill. The product from the rod mill was then screened and the material in the largest size fraction was separated into approximately ten density increments using a wet shaking table. Samples were taken at random times from the two flowing streams exiting the shaking table namely; concentrate (consists of more dense material) and tailings (consists of less dense material). These samples were then filtered (to get rid of excess water), dried and their densities measured by a pycnometer.

4. RESULTS AND DISCUSSION

This chapter discusses the results obtained by the methods described in chapter 3. The results are presented and discussed in three sections as follows:

- 4.1. Chemical characterization of slag which discusses the slag chemical composition determined by XRF powder pellet analysis technique.
- 4.2. Characterization of entrained alloy in slag which presents the calculated amounts of alloy entrainment and relates the entrainment to the process parameters.
- 4.3. Heterogeneity characterization which presents the method in which heterogeneity can be quantified and the extent to which heterogeneity nature of the slag may influence the analysis results.

4.1. Chemical characterization of slag

Slag samples (from furnace 3 and furnace 6) were analyzed by XRF on pressed powder pellets (described in chapter 3). As described in chapter 3, the pellets were prepared from both the oxidized samples and those samples in which the metal droplets were selected out (this was done to compare the results of the two differently prepared samples as the latter is what is done in the industry laboratory). Three pellets of the same sample were analyzed individually for each an every sample to access repeatability (or precision).

All the analysis results are presented in Tables 7.1 and 7.2 of Appendix A. Oxidizing the samples containing entrained alloy particles has been found to have a significant impact on FeO concentration, as it can be seen in the summarized FeO results in Figure 4.1. An increased concentration of FeO resulted from the oxidized samples as compared to the samples with no / few alloy particles or the non-oxidized samples. This is understandable as the alloy particles may contain a significant amount of Fe which would not been analyzed for if the alloy particles have been selected out. On the other hand, where no removal of entrained particles took place, the Fe (and Cr) was under-reported due to much of the Fe mass associated with small areas (due to density of the alloy droplets).

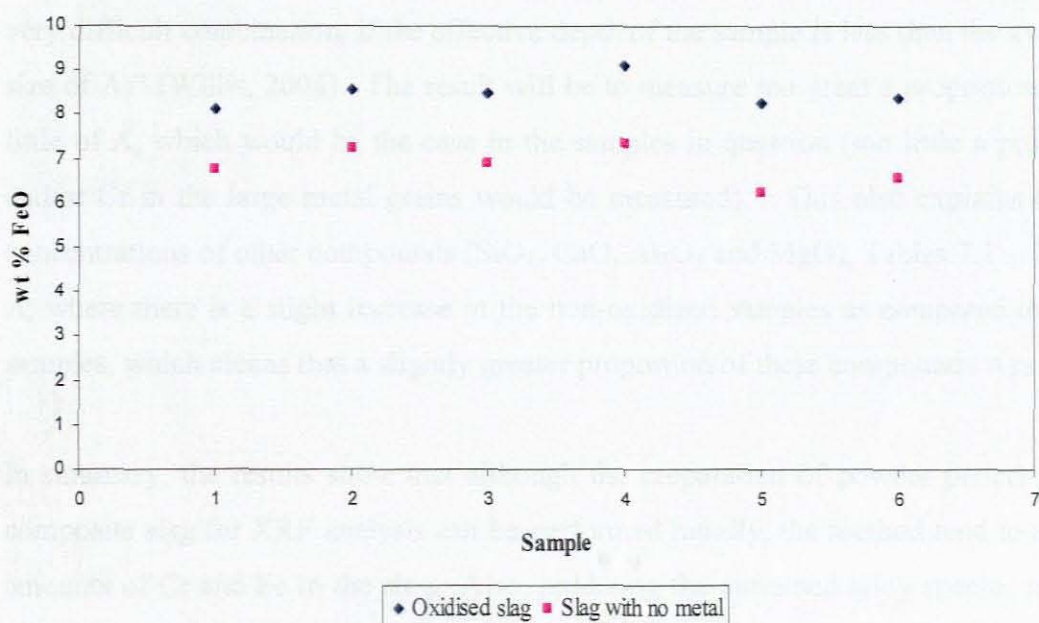


Figure 4. 1: FeO concentration in various slag samples

Few samples pulverized with alloy particles (entrained alloy particles not selected out and not oxidized), were analyzed and the results obtained for FeO were similar to those obtained in samples with no alloy particles (see Table 7.3 in Appendix A). A similar relationship has been observed for Cr_2O_3 although the difference in the results for differently treated samples was not as significant as it was for FeO.

A quantitative spot analysis of the alloy particles in slag was done using SEM-EDS and INCA software, to obtain the elemental composition of these particles. The results showed that about 85% in the entrained alloy particles is Fe which then explains a significant increase in FeO concentration once the slag has been oxidized (i.e. about 85% of the alloy is being oxidized to FeO).

The fact that the results of the samples analyzed with alloy particles showed low concentrations of FeO and Cr_2O_3 (compared to oxidized samples) can be attributed to the spectrometer not detecting the alloy particles in these samples. The reason for this is that XRF is a surface based method which requires a perfectly flat, smooth and homogeneous sample as during exposure *X-rays only penetrate a few microns layer*, depending on the sample composition. These requirements could not be met because of the grain size problem resulted from the fact that the entrained alloy species do not pulverize or grind well, they tend to deform rather than decrease in size during pulverization of composite slag.

“The *penetration depth* (of X-rays) is largely influenced by compounds of different particle sizes in a sample (i.e. large grains of compound A and small grains of compound B can be a

very difficult combination, if the effective depth of the sample is less than the average particle size of A)” (Willis, 2004). The result will be to measure too great a proportion of B and too little of A, which would be the case in the samples in question (too little a proportion of Fe and/or Cr in the large metal grains would be measured). This also explains the change in concentrations of other compounds (SiO_2 , CaO , Al_2O_3 and MgO), Tables 7.1 – 7.3, Appendix A, where there is a slight increase in the non-oxidized samples as compared to the oxidized samples, which means that a slightly greater proportion of these compounds was measured.

In summary, the results show that although the preparation of powder pellets of pulverized composite slag for XRF analysis can be performed rapidly, the method tend to understate the amounts of Cr and Fe in the slag. Also, oxidizing the entrained alloy species to their oxides before powder pellet preparation, lead to a much more homogeneous surface.

The ICP analysis performed at the plant laboratory on the other hand, including the dissolution stage can be regarded correct as the appropriate solution and calibration standards are used (these are described in chapter 2). The only problem with the method, besides that of turnaround time, is the removal of the entrained material during sample preparation (also described in chapter 2) which leads to biased, non-representative samples, and therefore inaccurate analysis results and mass balances. With the XRF method used in this work, the oxidized samples are not biased and so, in order to assess the accuracy of its results, it was appropriate to analyze the same oxidized samples on ICP using the plant laboratory’s dissolution procedure. The results of the two methods are compared in Table 4.1 in terms of component ratios (1, 2, 3 refer to the samples, 26-01F₃t₁SS₁, 02-02F₆t₂SS₁ and 04-02F₆t₃SS₂ respectively).

Table 4. 1: Comparison of results of XRF and ICP

	Cr/Fe ratio		Error	Fe/Si ratio		Error	Si/Mg ratio		Error	Mg/Al ratio		Error
	XRF	ICP		XRF	ICP		XRF	ICP		XRF	ICP	
1	0.627	1.696	1.069	0.589	0.623	0.035	0.873	0.785	0.088	2.066	0.868	1.197
2	0.686	1.958	1.272	0.629	0.644	0.016	0.959	0.821	0.137	1.979	0.869	1.109
3	0.659	1.695	1.036	0.562	0.661	0.099	0.871	0.773	0.098	1.970	0.832	1.138

For some of the components, large errors are evident and some show small errors. The errors may be due to the errors introduced during the sub-sampling stages, as a result of

heterogeneity (refer to section 4.3). It is possible therefore that the analysis sub-samples were not identical.

As mentioned earlier, repeatability (or precision) was assessed by analyzing three pellets of the same sample and the results in Table 7.1, appendix A show insignificant variations between individual pellets.

4.2. Characterization of entrained alloy in slag

Slag and alloy samples from the plant were analyzed by pycnometer to determine their densities which were then used in conjunction with equation 2.4, to calculate the mass fraction of the entrained alloy in slag. The density of the non-alloy slag used in all the calculations was estimated (using the model described in section 2.1.4.1) as 2.98 g/cm^3 . The results are tabulated in Table 4.2 (see Appendix A, section 7.2 for detailed calculations).

Table 4. 2: Alloy entrainment in various slags (non-alloy slag density = 2.98 g/cm^3)

Sample ID	Measured Density, g/cm^3		Total amount of entrained alloy	
	Slag	Alloy	Weight fraction, x	wt %
24/01F3t1SS3	3.40	6.71	0.222	22.2
26/01F3t1SS1	3.46	6.57	0.256	25.6
27/01F3t1SS2	3.35	6.56	0.204	20.4
03/02F6t1SS1	3.32	6.71	0.186	18.6
04/02F6t3SS2	3.40	6.65	0.224	22.4
02/02F6t2SS1	3.38	6.23	0.227	22.7

Figure 4.2 shows the relationship between the amount of entrained alloy in slag (wt %) and the density of slag as tapped from the plant (composite).

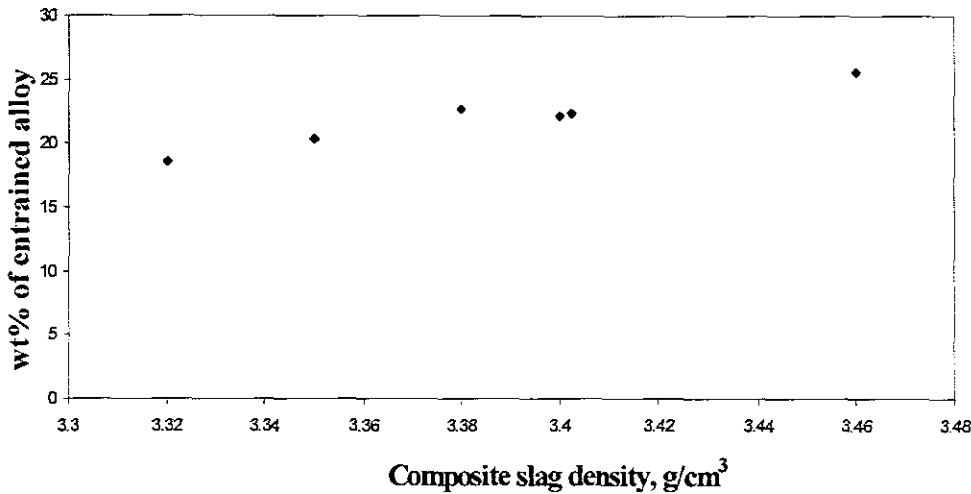


Figure 4. 2: Relationship between slag density and the amount entrained

The amount of entrainment increases with an increase in composite slag density and appears in significant proportions. The significant losses were also proven to be evident when a significant loss of density occurred after oxidizing the actual slag (density reduced from 3.35 g/cm³ to 2.83 g/cm³), indicating that significant oxidation did take place, which could only have happened if a significant proportion of the metal is in entrained form. This then shows that the main loss mechanism is through physical entrapment rather than chemical dissolution, which can also be seen in Figure 1.2 in chapter 1, and that a more fluid slag might lead to lower alloy losses to the slag.

The method used in this work, for calculating the weight percent of entrained alloy would be a useful tool for when performing mass balance calculations. Also, since the alloy entrainment in slag is largely influenced by the process parameters (such as viscosity, slag chemistry, temperature), the method would be useful for process control especially to determine if significant entrainment occurs (which is the case for the samples characterized here).

Slag viscosity is the most important property of chromium containing slags which governs the reduction process, and is also influential during tapping of the furnace. According to literature (Rennie, Howat and Jochens, 1972), small droplets of metal occur in the slag as a result of turbulence both in the furnace and when the furnace is tapped, and the rate at which these metal droplets are separated from the slag phase is a function of slag viscosity (i.e. to facilitate separation, viscosity needs to be as low as possible). Low slag viscosity is also essential for rapid mass transfer, and thus, for the whole process. Also refer to chapter 2, equation 2.3.

The literature reveals that it is extremely difficult to measure the viscosity of chromium containing slags simple because of high melting points and that chromium appears in two oxidation stages. Although there are ongoing attempts to develop models to predict viscosity (Forsbacka and Hollapa, 2004), these are not yet viable in industry and thus, the most viable approach to reducing metal entrainment to slag is by controlling the parameters that influence viscosity. These are slag chemistry (i.e. basicity, $\text{MgO}/\text{Al}_2\text{O}_3$ ratio), and the operating temperature, which have been discussed in detail in chapter 2. It is shown in chapter 2 that the amount of Cr entrainment decreases with an increase in slag basicity (Figure 2.1), and this is because the slag viscosity decreases as the slag basicity increases. Similarly, the slag viscosity decreases as the temperature increases.

The latter discussion is intended to show the importance of knowing the amount of entrainment in maintaining the effective performance of the process. The ability to quickly measure this amount would give the metallurgist an indication of the deviations in the process, and the slag chemistry information (say from XRF) would indicate necessary steps required to rectify the problem. The ability to measure the amount of entrainment would also be beneficial for metallurgical accounting, as the amount can now be included in mass balance calculations.

4.3. Heterogeneity quantification

It should be noted that the slag samples characterized here were not the same samples as those used for XRF analysis and alloy entrainment characterization. More samples had to be requested from Ferrometals as the first batch ran out and the second batch used for heterogeneity characterization was from a different furnace (furnace 4).

Heterogeneity was quantified using equation 2.15 which calculates what is called the sampling constant, K_s (Lyman defines the sampling constant as the direct measure of intrinsic heterogeneity and Gy (1982) refers to it as the constitutional heterogeneity). The sampling constant has the units of mass. The equation used required the knowledge of size and density distributions, and the subsequent sections discuss the results of these as well as the calculations performed. Knowledge of the sampling constant enables the calculation of the relative standard deviation (RSD), for a given sample mass.

4.3.1. Size distribution(s) of entrained alloy in slag

The size distributions of the entrained alloy in slag for slag samples (sampled from five consecutive taps) are shown in Figure 4.3, (a) represented in terms of number percent and (b) in terms of number of counts. Figure 4.4 shows an example of the BSE image from which alloy particles, appearing in white spherical phases, were measured, counted and classified into their respective size classes. The image is one of the images taken from a specimen (specimen A) of the sample tapped from the fifth tap (i.e. t5A). Images of all the samples can be found in Figures 8.1 to 8.4 in Appendix B.

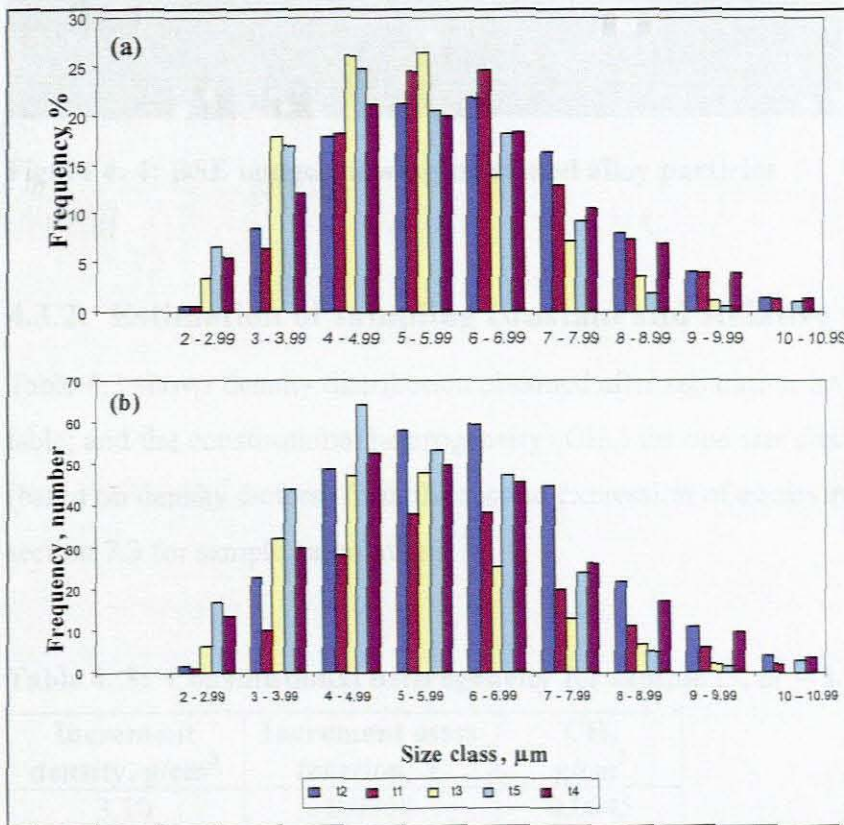


Figure 4. 3: Size distributions of alloy particles in ferrochrome slag

Figure 4.3 demonstrates that the entrained alloy particles in slag are in the size range 2 – 11 μm, with the particles in most samples falling within the range 3 – 7 μm (the results show that this was a good slag, i.e. no significant entrainment).

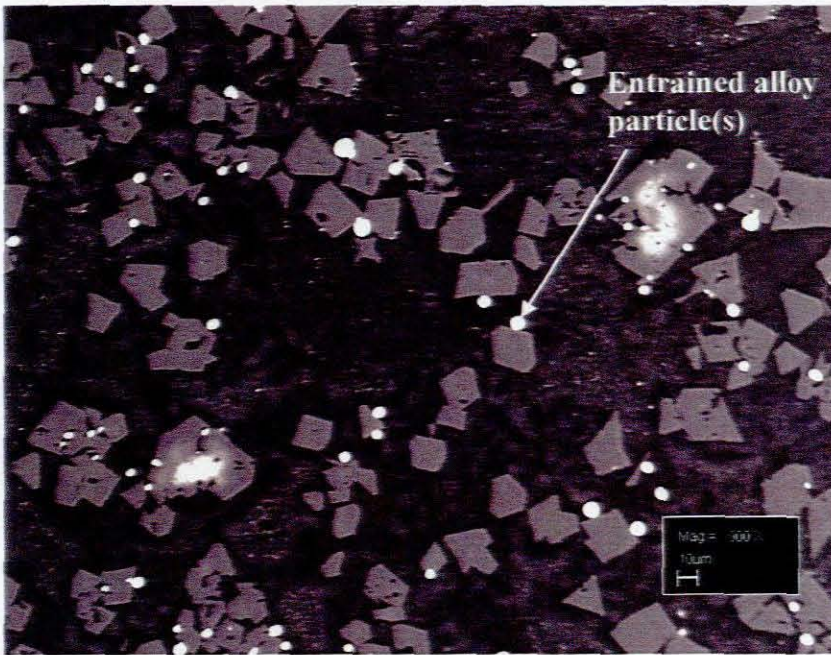


Figure 4. 4: BSE image showing entrained alloy particles

4.3.2. Estimation of sampling constant and Relative standard deviation

Table 4.3 shows density distribution obtained after separation into increments using a shaking table; and the constitutional heterogeneity (CH_v) for one size fraction of sample t3, calculated (based on density factors) from the second expression of equation 2.15. Refer to Appendix A, section 7.3 for sample calculations.

Table 4. 3: Constitutional heterogeneity for sample t3, $a_L = 8.63\%$

Increment density, g/cm^3	Increment mass fraction, Y	CH_v g/cm^3
3.10	0.0358	0.0045
3.20	0.0615	0.0363
3.00	0.1166	0.2397
3.12	0.1188	0.0012
3.12	0.0692	0.0014
3.06	0.0552	0.0311
3.02	0.1790	0.2904
3.11	0.3371	0.0152
3.43	0.0269	0.2963
Sum, $CH_v =$		0.9162

Using the calculated CH_v , the sampling constant was then calculated based on size factors (first expression of equation 2.15; the results are tabulated in Table 4.4. The volume used is the average particle volume calculated by equation 2.17 (Hogg, 2003) and then multiplied by the average frequency of particles within a specific size range ($X_u V_u$, Table 4.4). The sum at the bottom of column five is then the sampling constant. The sampling constant value depends only on the properties of the material sampled and a different value must be calculated for each component (Lyman, 1986).

Table 4. 4: Constitutional heterogeneity (size factors), t3

Size class, μm	Average size, cm	Average Frequency, X_u	$X_u V_u$ cm^3	$X_u V_u CH_v$, g
7 – 7.99	0.0750	13	0.0029	0.0026
6 – 6.99	0.0650	25	0.0036	0.0033
5 – 5.99	0.0550	48	0.0042	0.0038
4 – 4.99	0.0450	47	0.0022	0.0020
3 – 3.99	0.0350	32	0.00072	0.0007
2 – 2.99	0.0250	6	0.00005	4.47E-05
Sum, $K_s =$				0.0125

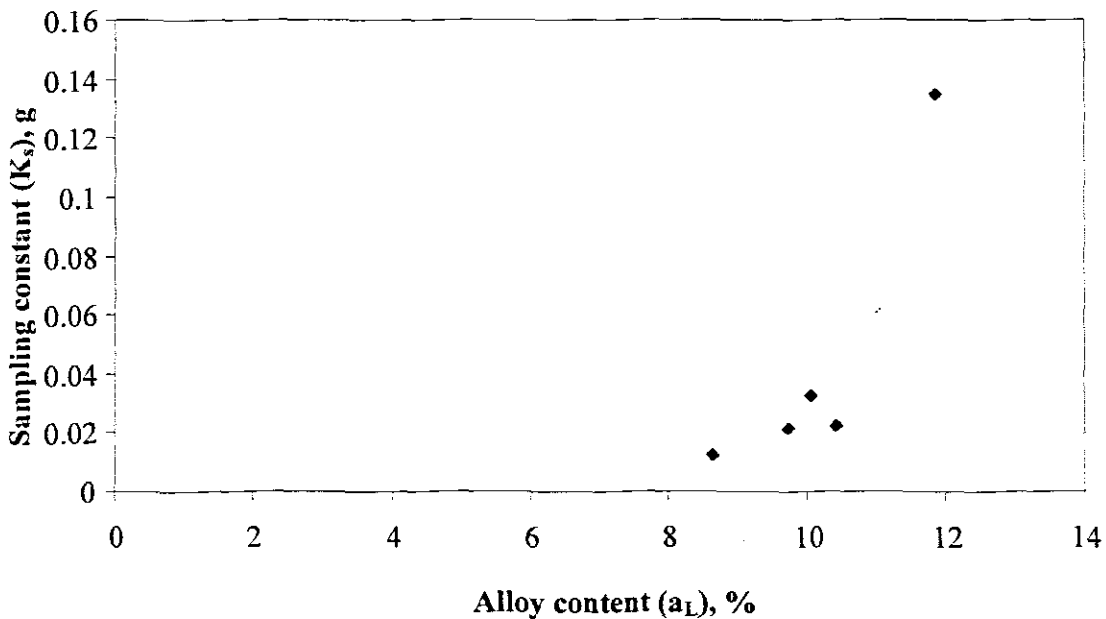
Relative standard deviation (%) = 0.335%, for sample mass, $M_s = 1109.3\text{g}$

Having calculated the sampling constant, the percent relative standard deviation (% RSD), expected as a result of constitutional heterogeneity in the treated sample was then calculated by equation 2.20 and was found to be 0.391% for the measured sample mass of 1109.3g. Multiple samples were treated in a similar way, experimental and calculated results for these are presented in Appendix A, Tables 7.4 – 7.11, and Table 4.5 below is a summary of calculated results obtained for the sampling constants and % RSD's.

Table 4. 5: Sampling constants and relative errors for five consecutive taps

Sample	Sampling constant, K_s	RSD %	Alloy content, %
t3	0.0125	0.335	8.63
t5	0.0212	0.774	9.72
t2	0.1347	0.986	11.85
t1	0.0222	0.512	10.42
t4	0.0324	0.514	10.06

The obtained % RSD's for various samples were found to be small and inconsistent on a sample by sample basis, showing that within a lot or a sample, the slag might have a low heterogeneity but between lots / samples there is significant variation. This implies that heterogeneity varies significantly throughout the furnace. The small values of the % RSD with respect to the entrained alloy were expected because, as is shown in Figure 4.4, the entrained alloy particles appear in very small sizes of narrow distributions. The inconsistency in the sampling constant values can be attributed to the variations inherent to the smelting process itself. This is shown in Figure 4.5 where the sampling constant increases with an increase in the amount of alloy entrained in slag, implying that the more alloy is entrained in slag, the more heterogeneous the slag becomes.

**Figure 4. 5: Sampling constant for samples from five consecutive taps**

The latter further implies that if we were to measure the sampling constant in the slag samples used in the initial work (XRF analysis and alloy entrainment determination), for which the calculated entrained alloy content was within the range 18 – 25 %, higher values of sampling constant and therefore % RSD would be obtained. This is also confirmed by Figure 1.2 in chapter 1, which shows larger particles of entrained alloy (note that the scale is 100 μm) in those samples compared to the samples characterized here (Figure 4.4, scale – 10 μm). Also, in Figure 1.2 a much wider distribution is observed which would again relate to high sampling constant values and % RSD, and means that the heterogeneity nature of those samples might have a significant impact on the final analysis results. This then explains the errors obtained when comparing XRF and ICP results (Table 4.1).

In summary, the sampling constant or intrinsic heterogeneity is strongly dependent on the entrained alloy content in slag, which in turn is strongly related to the process (see section 4.2). Thus, a step towards controlling the heterogeneity effect to an acceptable value for metallurgical accounting purposes would be to control the alloy entrainment in slag. This could be achieved through knowing the possible causes of entrainment, understanding as to how these causes influence entrainment and then taking the necessary steps towards solving the problem. These have already been discussed in section 4.2.

5. CONCLUSIONS AND RECOMMENDATIONS

The objectives of this study, as stated in the introduction were:

- To investigate if an accurate, robust and precise technique could be developed for ferrochrome slag (and alloy) analysis, and if this alternative technique would allow rapid turnaround times of samples analysis.
- To investigate if a density based method could be used in conjunction with a simple robust model, to estimate the amount (%) of entrained metal in slag.
- To quantify errors associated with the heterogeneity of ferrochrome slags so that the contribution of these errors to the overall sampling and analysis variance is understood.

The main objective for investigating the XRF analysis technique was to find out if it can be used to improve the turnaround times at the plant laboratory. It was apparent that the turnaround times were largely influenced by the long sample preparation procedures associated with the ICP technique. It was found that the XRF analysis of the composite slag by pressed powder pellets could be performed a bit quicker although improvement was insignificant (this is based on the procedure described in paragraph 2 of page 42, and refers to the samples that were not pretreated neither by selecting entrained alloy particles nor by oxidation), but because of the grain size effects resulted from the entrained alloy particles which could not pulverize well, the results were not accurate (refer to the discussion from paragraph 1 of page 47 to paragraph 2 of page 48). An extra stage in the sample preparation was then introduced, which included oxidation of the entrained alloy particles and this prolonged the turnaround times by about 16 hours. However, it is advised that a relatively large sample is pulverized and heated in pure oxygen at 1100 – 1200 °C in a zirconia crucible as this will speed up the oxidation process and possibly improve the turnaround times. It will also minimize errors that might be introduced during sub-sampling as it would be much easier to obtain a representative sub-sample from a large homogenized sample. Another factor contributed to the insignificant improvement of turnaround time is the type of binder used (mixed with the samples before they are pressed) which required some time to dry the samples. Other types of binders could be investigated which are in powder form and therefore do not require drying.

It was demonstrated that the stage in the sample preparation practice at the plant laboratory, which involves selecting the best appearing pieces of the “tapped” slag sample, after it has been crushed, leads to analysis results that are not accurate. The method used in this work therefore, of oxidizing the entrained alloy particles does not necessarily have to be used only for powder pellet preparation for XRF analysis. It is advised that this method (as stated in the preceding paragraph) be practiced during sample preparation at the plant laboratory even if the samples are to be analyzed by the ICP.

The percentage of the entrained alloy in some slags studied is in the range 18 – 25% (according to different samples analyzed). The entrainment is therefore much greater than is recovered on the reclamation plant (around 2%). This also means that physical rather than chemical factors have to be controlled in the furnace melts. Based on the findings it can be concluded that a rapid estimation of alloy entrainment is possible using a robust technique such as a pycnometer, which may even be situated in the control room in the plant. It takes a maximum of about 8 minutes to obtain the density results of one sample, including all the preparations involved, using a manual pycnometer device. With an automatic device, this time could improve significantly. However, some validation still needs to be done to check the reliability of the pycnometer results before implementing this method. One possible validation method would be the one described by Viana, Jouannin, Pontier and Chulia (2002).

A quantitative measure of heterogeneity (sampling constant) was done based on the entrained alloy in slag and was found to increase with an increase in the entrained alloy content in slag. For the later slag samples characterized (compared to the slag shown in Figure 1.2) it was found that heterogeneity contributes insignificantly to the overall sampling and analysis variance and therefore the final analysis results. This was based on the calculated relative standard deviations (on sample by sample basis) which were very small such that it could be assumed that errors due to heterogeneity are negligible. However, the samples on which this observation is based had little alloy entrained in them (i.e. 8 – 11 %) implying that the furnace (furnace 4) from which they were tapped was performing well. This is in contrast to the entrainment of 18 – 25 % obtained in the samples tapped from furnaces 3 and 6, and since the sampling constant increases with the entrained alloy content, higher relative standard deviations would be expected. Thus, the effect of heterogeneity based of the entrained alloy in slag is dependent on the process as much as the entrainment is.

As the sampling constant depends on all the individual components of the material sampled (Lyman, 1998 and Gy, 1982), it is recommended that its measurement done based on other components of the slag as well.

For furnaces it can therefore be said that for a given sample mass, the sampling constant and the variance are not static, but they are dynamically dependent on operating conditions, especially the slag viscosity. Moreover, this heterogeneity that results from process conditions also influence the accuracy of subsequent assaying practice, be it XRF or ICP. Finally, one can say that rapid estimation of entrainment will aid in mass balancing the furnace and allow one to gauge the reliability of the analysis results.

6. REFERENCES

1. A handbook of fusion methods: *The preparation of Fused Glass Beads*, Retrieved: September 06, 2004, from <http://www.aft-fusion.com/fusionmethods.htm>
2. Assibey-Bonsu, 'Summary of present knowledge on the representative sampling of ore in the mining industry', *Journal of the South African Institute of Mining and Metallurgy*, November 1996.
3. Banda, W., 'Pyrometallurgical recovery of Cobalt from waste reverbaratory furnace slag by DC plasma arc furnace technology', Chapter 3, Unpublished Masters Thesis, University of Stellenbosch, Stellenbosch, 2001.
4. Barcza N.A., Curr T.R., Winship W.D. and Heanly C.P., 'The production of ferrochromium in a transferred arc plasma furnace', *Proceedings of the 39th Electric arc furnace conference*, Houstonm Iron and Steel Society of the AIME, pp. 243 – 260, 1981.
5. Bartlett H., 'Mass balances across F2, F3 and F6 – Preliminary report', Unpublished report, Hugh Bartlett Consulting CC., Johannesburg, August 2003.
6. Bower N.W., Neifert P.E. and Lewis C.M., 'Minimizing the sources of error in the analysis of geological samples by X-ray fluorescence', *The Rigaku journal* 7, pp. 3-21, 1990.
7. Carrasco P., Campos M, Tapia J. and Menichetti E., 'Heterogeneity and Ingamells's tests of some Chilean Porphyry ores', *Sampling and Blending conference proceedings*, Sunshine Coast, QLD, pp. 139 – 150, 9 – 12 May 2005.
8. Eksteen J.J., 'A generic, semi-empirical approach to the stochastic modelling of bath-type pyrometallurgical reactors', Unpublished PhD Thesis, University of Stellenbosch, Stellenbosch, 2003.
9. Forsbacka L. and Holappa L., 'Viscosity of CaO – CrO – SiO₂ slags in a relatively high oxygen partial pressure atmosphere', *Scandinavian Journal of Metallurgy* 33, pp 261 – 268, 2004.
10. François-Bongarçon D. and Gy P., 'The most common error in applying Gy's formula in the theory of mineral sampling, and the history of the liberation factor', *Journal of the South African Institute of Mining and Metallurgy*, pp. 475 – 479, November / December 2002.

11. François-Bongarçon D. and Gy P., 'Critical aspects of sampling in mills and plants: a guide to understanding sampling audits', *Journal of the South African Institute of Mining and Metallurgy*, pp. 481 – 484, November / December 2002.
12. Geelhoed B., 'A generalisation of Gy's model for the fundamental sampling error', *Sampling and Blending conference proceedings, Sunshine Coast, QLD*, pp. 19 – 25, 9 – 12 May 2005.
13. Gerlach R.W. and Nocerino J.M., 'Guidance for obtaining representative laboratory analytical sub-samples from particulate laboratory samples', *United States Environmental Protection Agency, EPA/600/R-03/027*, November 2003.
14. Goto, A. and Tatsumi Y., 'Quantitative analysis of rock samples by an X-ray fluorescence spectrometer (II)', *The Rigaku Journal* 13, pp. 20-39, 1996.
15. Gy P.M., 'Sampling of particulate materials: Theory and practice', 2nd ed., Elsevier, Amsterdam, 1982.
16. Harding D.P., 'Mineral identification using a scanning electron microscope', *Journal of Minerals & Metallurgical Processing*, 19 (4), pp. 169 – 177, November 2002.
17. Hayes P.C., 'Aspects of SAF smelting of ferrochrome', *Tenth International Ferroalloys Congress, Cape Town, South Africa*, pp. 1 – 14, 1 – 4 February 2004.
18. Hogg R., 'Characterization of relative homogeneity in particulate mixtures', *International journal of mineral processing* 72, pp. 477 – 487, 2003.
19. Holappa L. and Xiao P., 'Slags in ferroalloys production – review of present knowledge', *Proceedings of VII International Conference on Molten Slags, Fluxes and salts*, pp. 641-649, 2004.
20. Jansson A., Brabie V., Fabo E. and Jansson S., 'Slag formation and its role in the ferrochromium production', *Scandinavian Journal of Metallurgy* 31, pp 314 – 320, 2002.
21. Keene B.J. and Mills K.C., 'Densities of molten slags', in D. Springorum (2nd ed.), *Slag Atlas*, Dusseldorf, 1995.
22. La Tour T.E., 'Analysis of rocks using X-ray fluorescence spectrometry', *The Rigaku Journal* 6, pp 3 – 9, 1989.
23. Lyman, G.J., 'The influence of segregation of particulates on sampling variance – the question of distributional heterogeneity', *International Journal of Mineral Processing* 55, pp. 95 – 112, 1998.
24. Lyman G.J., 'Application of Gy's sampling theory to coal: a simplified explanation and illustration of some basic aspects', *International Journal of Mineral Processing* 17, pp. 1 – 22, 1986.

25. Mills K.C. 1995. Viscosities of molten slags. In Springorum D. (2nd Ed.). Slag Atlas. Dusseldorf.
26. Mori P.E., Reeves S., Correia C.T., Haukka M., Development of a fused glass disc XRF facility and comparison with the pressed powder pellet technique at Instituto de Geociencias, SAO Paulo University. Revista Brasileira de Geociencias, volume 29, 1999.
27. Muan A., Slag – Metal equilibrium involving chromium as a component, MINTEK 50, Sandton, 1984, p897 – 904.
28. Nuspl M., Wegscheider W., Angeli J., Posch W. and Mayr M., ‘Qualitative and quantitative determination of micro-inclusions by automated SEM/EDX analysis’, Special issue paper, Anal Bioanal Chem 379, pp. 640 – 645, 2004.
29. Petruk W., ‘Imaging of minerals, ores and related products to determine mineral characteristics’, Journal of Minerals & Metallurgical Processing 19 (1), pp. 50 – 56, February 2002.
30. Pitard F.F., ‘Pierre Gy’s sampling theory and sampling practice: Heterogeneity, Sampling Correctness and Statistical Process Control’, 2nd ed., CRC Press, Boca Raton, New York, 1993.
31. Qiao Z and Xiaomin T, ‘X-ray Fluorescence spectrometry determination of chromite by powder briquette pressed technique’, Proceedings of the 65th World Foundry Congress, Gyeongju, Korea, pp. 1161-1167, 2002.
32. Rennie M.S., Howat D.D. and Jochens P.R., ‘The effects of chromium oxide, iron oxide and calcium oxide on the liquidus temperatures, viscosities and electrical conductivities of slags in the system MgO – Al₂O₃ – SiO₂’, Journal of the South African Institute of Mining and Metallurgy, August 1972.
33. Riekkola-Vanhanen M., ‘Finnish expert report on best available techniques in ferrochromium production’, The Finnish Environment 314, Edita Ltd, Helsinki, June 1999.
34. Rousseau R.M., ‘Detection limit and estimate of uncertainty of analytical XRF results’, The Rigaku Journal 18 (2), pp. 33 – 47, 2001.
35. Schuchardt K. and Schymik R., ‘Laboratory information and management systems’, Ullmann’s Encyclopedia of Industrial Chemistry B6, pp. 307 – 315, 1994.
36. Sear L.G., ‘The fusion of difficult materials including Chromite, Cassiterite and reduced Sulphur’, X-ray Spectrometry 26, pp. 105 – 110, 1997.
37. Sowmya T. and Sankaranarayanan S.R., ‘Spectroscopic analysis of slags – preliminary observations’, Proceedings of VII International Conference on Molten Slags, Fluxes and salts, pp. 693-698, 2004.

38. Tertian R. and Claisse F., 'Principles of quantitative X-ray fluorescence analysis', Heyden & Sons Ltd, London, 1982.
39. Viana M., Jouannin P., Pontier C., Chulia D., 'About pycnometric density measurements', *Talanta* 57 pp. 583 – 593, 2002.
40. Wedepohl A., 'The mineralogy of the reduction of chromium ore in a plasma furnace', *MINTEK* 50, Sandton, pp. 905 – 912, 1984.
41. Willis J.P., Theory and practice of XRF spectrometry, Cape Town: University of Cape Town, [Unpublished course notes], 2004.

7. APPENDIX A: RESULTS AND SAMPLE CALCULATIONS

7.1. XRF results

The following tables present the XRF analysis results.

Table 7. 1: XRF results of oxidized slag

Sample ID	Component concentration, wt %					
	Al ₂ O ₃	CaO	Cr ₂ O ₃	FeO	SiO ₂	MgO
24-01F ₃ t ₁ SS ₃	21.21	2.859	13.873	8.069	24.736	18.496
	22.487	3.146	13.968	8.161	26.196	19.296
	22.592	3.064	13.977	8.187	26.313	19.396
26-01F ₃ t ₁ SS ₁	22.92	2.891	12.135	8.498	23.362	21.012
	23.579	3.427	12.281	8.614	24.034	21.385
	24.67	2.851	12.218	8.612	25.264	22.112
27-01F ₃ t ₁ SS ₂	23.612	2.779	12.164	8.479	25.502	21.344
	23.137	2.782	12.195	8.465	25.098	20.947
	23.662	2.939	12.26	8.581	25.783	21.372
02-02F ₆ t ₂ SS ₁	22.872	4.096	14.137	9.086	24.525	19.781
	22.355	4.393	14.24	9.133	24.018	19.432
	22.117	4.424	14.185	9.104	23.756	19.247
03-02F ₆ t ₁ SS ₁	24.799	4.491	11.198	8.219	25.965	20.618
	26.579	4.441	11.346	8.350	27.957	21.831
04-02F ₆ t ₃ SS ₂	26.034	4.009	12.418	8.302	25.412	22.307
	25.972	4.488	12.623	8.417	25.216	22.381
	24.519	4.853	12.622	8.403	23.685	21.461

Table 7. 2: XRF results of non-oxidized slag, metallic particles selected out

Sample ID	Component concentration, wt %					
	Al ₂ O ₃	CaO	Cr ₂ O ₃	FeO	SiO ₂	MgO
24-01F ₃ t ₁ SS ₃	23.832	3.103	13.769	6.897	27.579	20.04
	22.872	3.193	13.694	6.816	26.348	19.507
	23.774	2.863	13.586	6.783	27.425	20.028
26-01F ₃ t ₁ SS ₁	26.117	2.887	12.256	7.203	26.032	22.745
	27.016	2.935	12.277	7.233	26.837	23.315
	26.638	3.153	12.34	7.273	26.461	23.074
27-01F ₃ t ₁ SS ₂	23.681	3.069	12.217	6.937	25.042	21.13
	24.521	2.683	12.165	6.935	26.061	21.621
	23.072	2.939	12.113	6.864	24.366	20.606
02-02F ₆ t ₂ SS ₁	22.412	4.343	14.23	7.462	24.151	19.096
	21.542	4.599	14.166	7.369	23.105	18.443
	21.463	3.902	13.919	7.213	23.043	18.423
03-02F ₆ t ₁ SS ₁	27.216	4.867	10.924	6.344	28.592	21.912
	26.374	4.796	10.893	6.286	27.656	21.286
	26.633	4.605	10.793	6.201	28.199	21.47
04-02F ₆ t ₃ SS ₂	27.358	4.561	12.702	6.659	27.276	22.906
	26.148	4.203	12.407	6.451	25.914	22.095
	27.549	4.615	12.663	6.595	27.39	23.084

Table 7.3: XRF results of slag pulverized with metal droplets

Sample ID	Component concentration, wt %					
	Al ₂ O ₃	CaO	Cr ₂ O ₃	FeO	SiO ₂	MgO
24-01F ₃ t ₁ SS ₃	25.24	4.21	12.47	6.35	24.48	21.29
26-01F ₃ t ₁ SS ₁	25.14	4.40	12.52	6.36	24.50	21.22
27-01F ₃ t ₁ SS ₁	25.78	4.34	12.59	6.42	25.11	21.71
02-02F ₆ t ₂ SS ₁	25.86	4.80	12.70	6.46	25.04	21.69
03-02F ₆ t ₁ SS ₁	25.51	4.51	12.61	6.41	24.74	21.37
04-02F ₆ t ₃ SS ₂	26.45	4.47	12.63	6.46	25.72	22.01

7.2. Calculation of alloy entrainment in slag

The weight fraction of the entrained metal in slag was calculated by equation 2.4. The sample calculation to follow is done for sample F3t1SS3 (row 3, Table 4.2). For this sample the densities of alloy and slag as “tapped” (ρ_m and ρ_{cs}) were measured as 6.71 and 3.40 g/cm³ respectively. The density of non-alloy slag (ρ_{cs}) was estimated as 2.98, and this value was used for the calculation of all the samples.

Thus,

$$\begin{aligned}
 x &= \frac{\rho_m(\rho_s - \rho_{cs})}{\rho_{cs}(\rho_s - \rho_m)} \\
 &= \frac{6.71(2.98 - 3.40)}{3.40(2.98 - 6.71)} \\
 &= 0.222
 \end{aligned}$$

$$\begin{aligned}
 \% \text{ entrained} &= 0.222 \times 100 \\
 &= 22.2\%
 \end{aligned}$$

7.3. Calculation of the sampling constant and RSD, %

The sample calculations to follow are for the results of sample t5 presented in tables 7.4 and 7.5 below. In table 7.4, columns 1 and 2 are the experimental results from which CH_v (3rd column) is calculated. CH_v is the heterogeneity based on density factors and is represented by the second expression of equation 2.15 as follows:

$$CH_v = \sum_{v=1}^{N_d} (\rho Y)_{increment} \frac{\left(\left(\frac{\rho_m (\rho_s - \rho_{increment})}{\rho_{increment} (\rho_s - \rho_m)} \right) \times 100 - a_L \right)^2}{a_L^2}$$

a_L is the average (total) alloy content in the bulk / composite slag, which is calculated using equation 2.4 as follows, where, ρ_m and ρ_s are 6.7 and 2.98 respectively.

$$\begin{aligned} a_L &= \frac{\rho_m (\rho_s - \rho_{cs,average})}{\rho_{cs,average} (\rho_s - \rho_m)} \times 100 \\ &= \frac{6.7(2.98 - 3.15)}{3.15(2.98 - 6.7)} \times 100 \\ &= 9.72\% \end{aligned}$$

CH_v for one increment (i.e. row 2, table 8.4) is then calculated as:

$$\begin{aligned} CH_{v,1} &= (\rho Y)_{increment1} \frac{\left(\left(\frac{\rho_m (\rho_s - \rho_{increment1})}{\rho_{increment1} (\rho_s - \rho_m)} \right) \times 100 - a_L \right)^2}{a_L^2} \\ &= 3.14 \times 0.185 \frac{\left(\left(\frac{6.7(2.98 - 3.14)}{3.14(2.98 - 6.7)} \right) \times 100 - 9.72 \right)^2}{9.72^2} \\ &= 0.0018 \text{ g/cm}^3 \end{aligned}$$

Similar calculations are performed for all the increments (i.e. CH_v , 2, 3, - 10) and the results (column 3) are summed up so that:

$$\begin{aligned} CH_v &= 0.0018 + 0.0717 + 0.0311 + 0.0848 + 0.0044 + 0.1878 + 0.0241 + 0.1195 + 0.3326 \\ &\quad + 0.1537 \\ &= 1.0116 \text{ g/cm}^3 \end{aligned}$$

Table 7.4: Constitutional heterogeneity (density factors) for sample t5, $a_L = 9.72\%$

Increment density, g/cm ³	Increment mass fraction, Y	CH _v , g/cm ³
3.14	0.185	0.0018
3.04	0.063	0.0717
3.09	0.098	0.0311
3.03	0.061	0.0848
3.12	0.053	0.0044
2.98	0.067	0.1878
3.20	0.114	0.0241
3.07	0.205	0.1195
2.95	0.076	0.3326
3.01	0.078	0.1537
Sum, CH_v =		1.0116

The sampling constant can now be written as (refer to equation 2.15):

$$K_s = \sum_{u=1}^{N_s} X_u V_u \cdot CH_v \text{ where, } V_u = \phi \alpha_u^3$$

ϕ is a shape factor which is equal to $\pi/6 = 0.5236$, assuming that the particles are spherical.

Then, for one size fraction (2nd row of table 8.5):

$$\begin{aligned} X_u V_u \cdot CH_v &= 24 \times 0.5236 \times 0.075^3 \times 1.0116 \\ &= 0.0054 \text{ g} \end{aligned}$$

Performing similar calculations for other size fractions yields values in the last column, and the sum of these values is the sampling constant, i.e.

$$\begin{aligned} K_s &= 0.0054 + 0.0069 + 0.0047 + 0.0031 + 0.0010 + 0.00014 \\ &= 0.0212 \text{ g} \end{aligned}$$

Table 7. 5: Constitutional heterogeneity (size factors), t5

Size class, μm	Average size, cm	Average Frequency, X_n	$X_n V_n$ cm ³	$X_n V_n CH_v$ g
7-7.99	0.0750	24	0.0053	0.0054
6-6.99	0.0650	48	0.0068	0.0069
5-5.99	0.0550	54	0.0046	0.0047
4-4.99	0.0450	65	0.0031	0.0031
3-3.99	0.0350	44	0.00098	0.0010
2-2.99	0.0250	17	0.00014	0.00014
Sum, $K_s =$				0.0212

Given the sample mass ($M_s = 353.9$ g, measured), the sampling constant value can then be used to calculate the % relative standard deviation:

$$\begin{aligned}
 RSD, \% &= \sqrt{\frac{K_s}{M_s}} \times 100 \\
 &= \sqrt{\frac{0.0212}{353.9}} \times 100 = 0.774\%
 \end{aligned}$$

Table 7. 6: Constitutional heterogeneity (density factors) for sample t2, $a_L = 11.85$ %

Increment density, g/cm ³	Increment mass fraction, Y	CH _v g/cm ³
2.81	0.0259	0.2745
3.06	0.0478	0.0517
3.17	0.0292	0.00064
3.19	0.0296	0.00004
2.83	0.0452	0.4258
2.96	0.0662	0.2335
3.02	0.1049	0.2099
3.01	0.0871	0.1837
3.61	0.2037	2.0373
3.11	0.3603	0.1387
Sum, CH_v =		3.5558

Table 7. 7: Constitutional heterogeneity (size factors), t2

Size class, μm	Average size, cm	Average frequency	$X_u V_u$ cm^3	$X_u V_u \text{CH}_v$, g
9 – 9.99	0.0950	11	0.0049	0.0175
8 – 8.99	0.0850	22	0.0071	0.0251
7 – 7.99	0.0750	45	0.0099	0.0353
6 – 6.99	0.0650	60	0.0086	0.0306
5 – 5.99	0.0550	58	0.0050	0.0179
4 – 4.99	0.0450	49	0.0023	0.0083
Sum, K_s =				0.1347

*Relative standard deviation (%) = 0.986 %, for sample mass, $M_s = 1383.9\text{g}$

Table 7. 8: Constitutional heterogeneity (density factors) for sample t1, $a_L = 10.42\%$

Increment density, g/cm^3	Increment mass fraction, Y	CH_v g/cm^3
3.20	0.1007	0.0114
3.21	0.0891	0.0163
3.33	0.1196	0.2658
3.18	0.0941	0.0023
3.12	0.1063	0.0167
3.05	0.0948	0.1041
3.06	0.0967	0.0888
3.12	0.0974	0.0153
3.31	0.1030	0.1784
3.25	0.0993	0.0613
Sum, CH_v =		0.7603

Table 7. 9: Constitutional heterogeneity (size factors), t1

Size class, μm	Average size, cm	Average frequency	$X_n V_n$ cm^3	$X_n V_n \text{CH}_v$ g
9 – 9.99	0.0950	10	0.0045	0.0034
8 – 8.99	0.0850	17	0.0056	0.0041
7 – 7.99	0.0750	26	0.0057	0.0044
6 – 6.99	0.0650	46	0.0066	0.0050
5 – 5.99	0.0550	50	0.0043	0.0033
4 – 4.99	0.0450	43	0.0025	0.0019
Sum, $K_s =$				0.0222

*Relative standard deviation (%) = 0.512 %, for sample mass, $M_s = 846.3\text{g}$

Table 7. 10: Constitutional heterogeneity (density factors) for sample t4, $a_L = 10.06\%$

Increment density, g/cm^3	Increment mass fraction, Y	CH_v g/cm^3
3.33	0.0816	0.2132
3.27	0.0942	0.1085
3.20	0.0942	0.0164
3.21	0.0914	0.0220
2.99	0.1027	0.2646
3.08	0.1181	0.0619
3.18	0.1111	0.0043
3.02	0.1125	0.1990
2.79	0.0802	1.0760
2.90	0.1139	0.7212
Sum, $\text{CH}_v =$		2.6869

Table 7. 11: Constitutional heterogeneity (size factors), t4

Size class, μm	Average size, cm	Average frequency	$X_u V_u$ cm^3	$X_u V_u C H_v$ g
7 - 7.99	0.0750	10	0.0022	0.0059
6 - 6.99	0.0650	20	0.0029	0.0077
5 - 5.99	0.0550	45	0.0039	0.0105
4 - 4.99	0.0450	48	0.0023	0.0061
3 - 3.99	0.0350	33	0.0007	0.0020
2 - 2.99	0.0250	8	0.0001	0.0002
Sum, $K_s =$				0.0324

*Relative standard deviation (%) = 0.514 %, for sample mass, $M_s = 1227.2\text{g}$

8. APPENDIX B: SEM BSE IMAGES OF SLAG

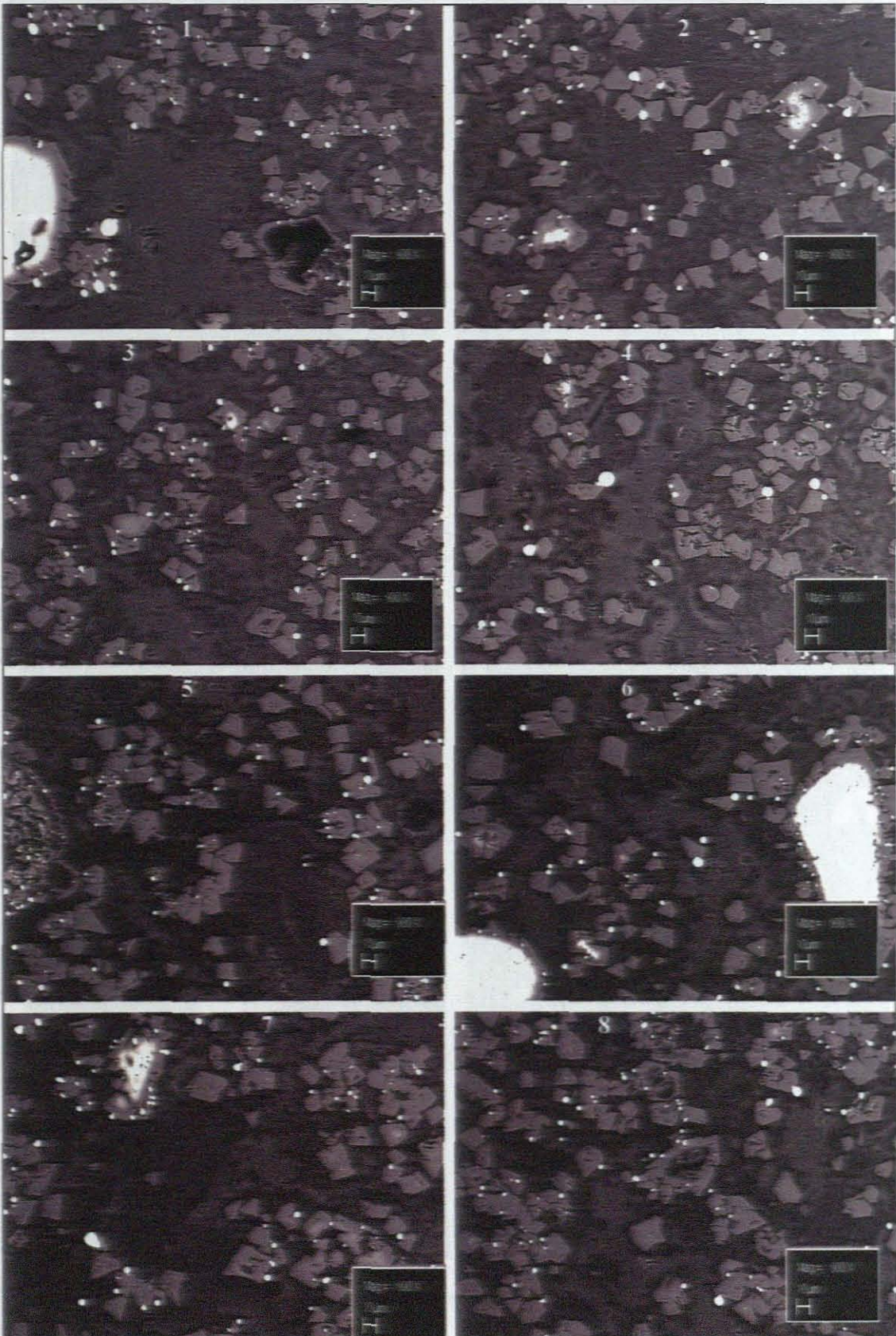


Figure 8. 1: T4A (1, 2, 3), T4B (4, 5, 6, 7, 8)

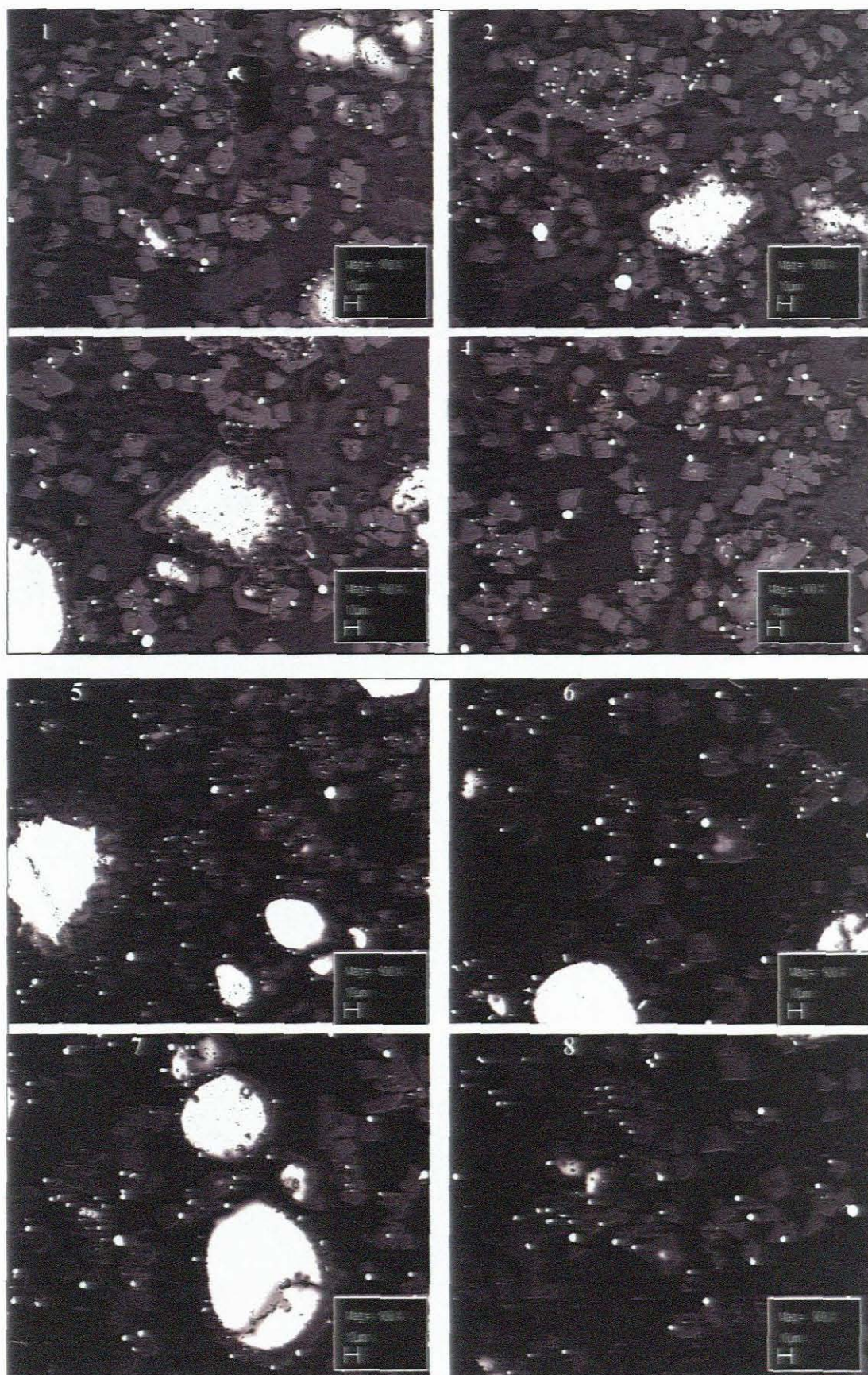


Figure 8. 2: T1A (1, 2, 3, 4), T1B (5, 6, 7, 8)

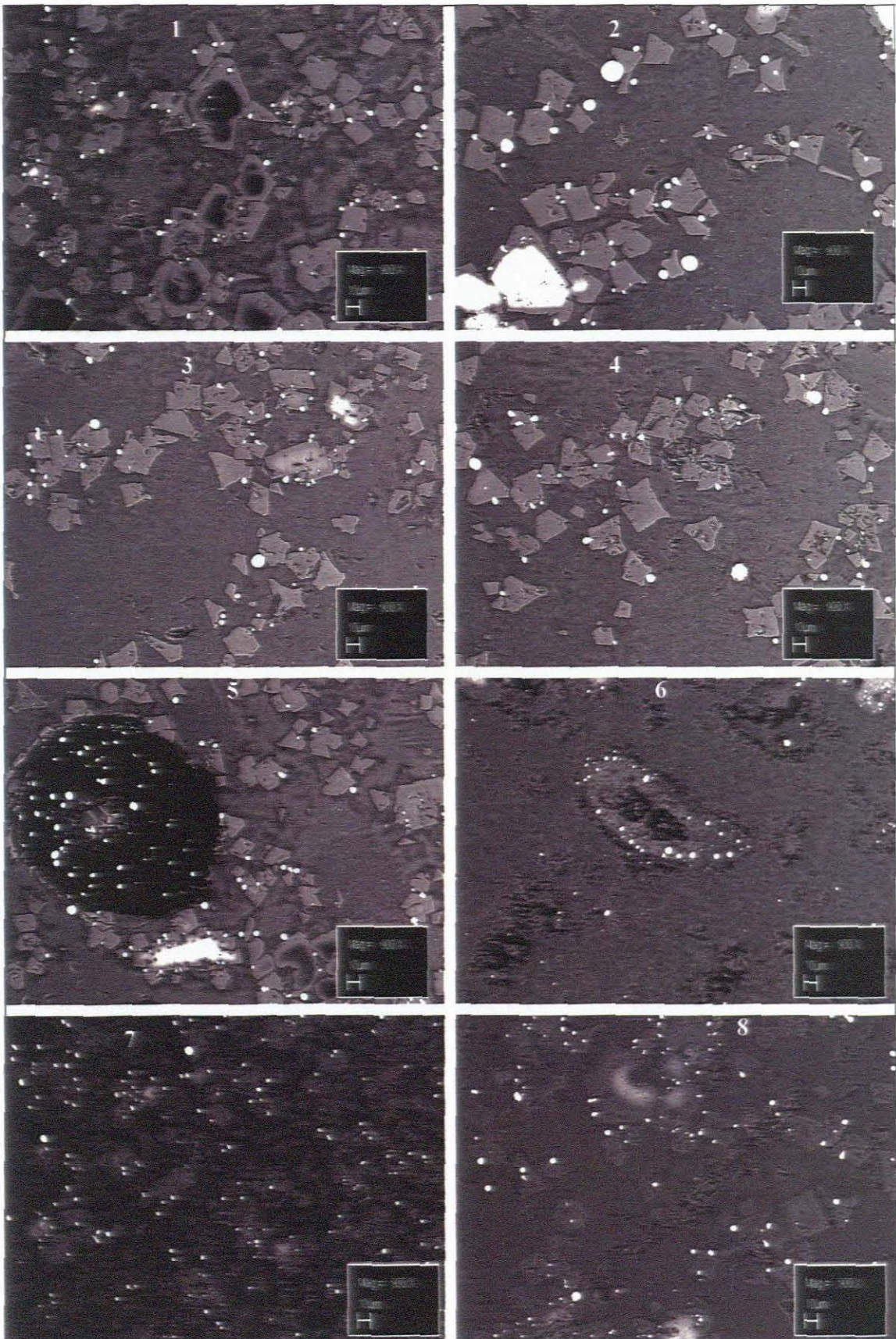


Figure 8.3: T2B (1), T2C (2, 3, 4), T2A (5), T3B (6, 7), T3C (8)

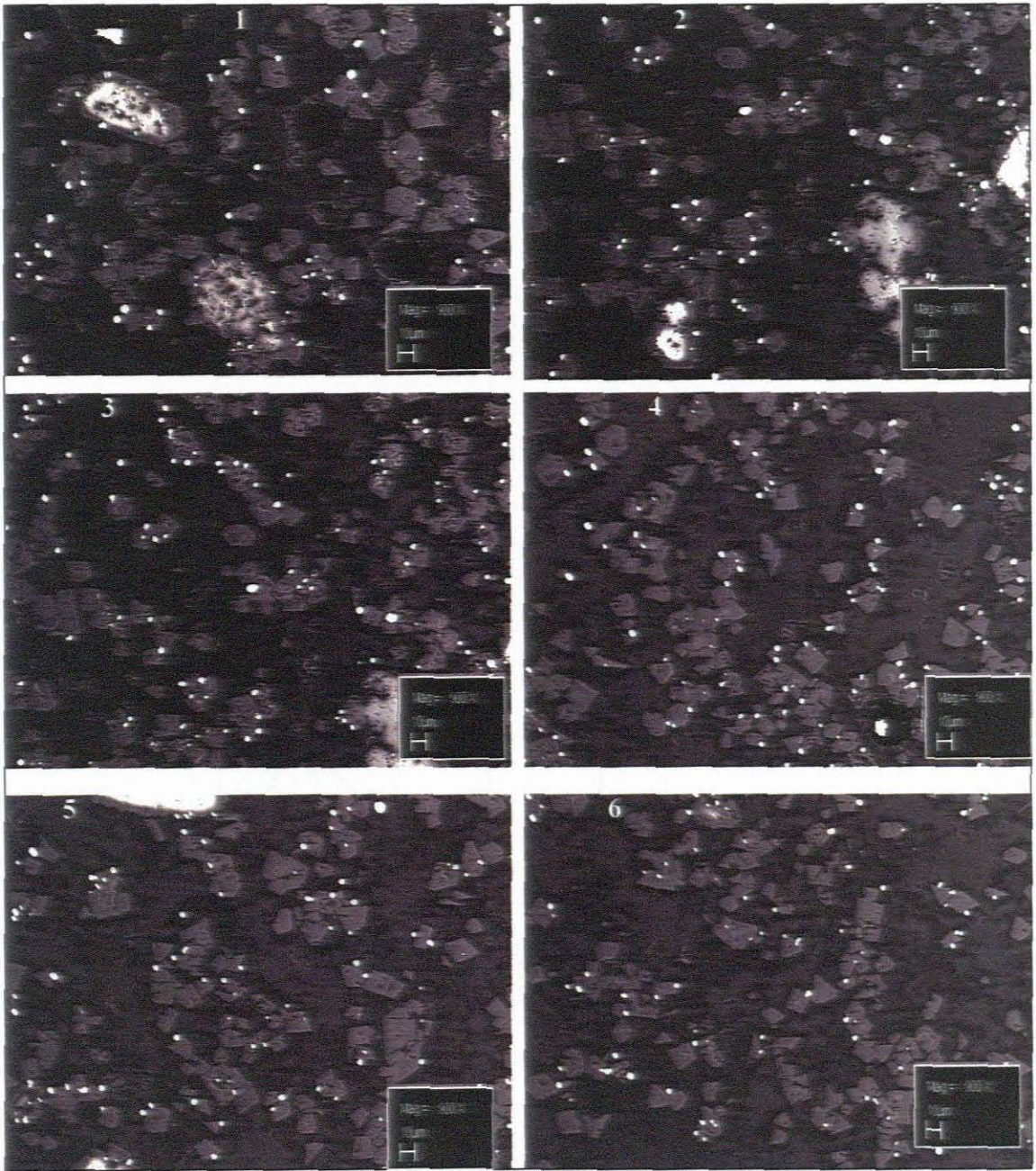


Figure 8. 4: T5A (1, 2, 3), T5B (4, 5, 6)

9. APPENDIX C: SAMPLING METHODS (Gerlach and Nocerino, November 2003)

9.1. Sectorial Splitter

A sectorial splitter consists of a rotating metal cone with ridges and valleys. The sectors should be radially symmetric and of equal size. The sample is placed in a hopper with adjustable vibration levels set such that the sample particles slowly emerge and fall onto the side of the rotating cone (Figure 10.1).

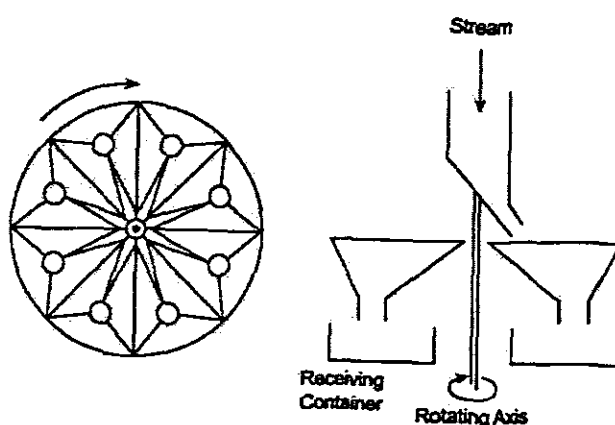


Figure 10. 1: A sectorial splitter with eight sectors

As the particles fall from the hopper, they are sometimes channelled through a funnel before dropping onto the side of the rotating cone. The hopper should be just above the funnel or cone to minimize loss from bouncing off the apparatus. Particles fall into containers placed under each valley. The receiving vessels depend on the size and design of the splitter. Small splitters may use a test tube while large splitters may require beakers or jars. The best results are obtained when operating the sectorial splitter with a constant rotational velocity and feeding it at a constant rate. Slow feed rates increase the number of increments and help to minimize the grouping and segregation error.

9.1.1. Advantages of a sectorial splitter

Sectorial splitters have several positive attributes. There is little extraneous between particle correlation allowed to propagate from the sample to the sub-sample. The increment size is

small irrespective of any segregation due to processes at work in the hopper and container, and only a small amount of sample is presented to the splitter at any time. Thus, because of those many increments, the grouping and segregation errors are small. Since the entire sample is processed, the delimitation and extraction errors are negligible as well. The only significant error is the fundamental error (assuming no gross operation errors). Related to the lack of correlation, one finds that different particle sizes tend to emerge independently of each other. Sectorial splitters remove virtually all the uncertainty associated with operator bias and require very little time from the analyst.

9.2. Incremental sampling

An increment is a group of particles or material physically extracted from the lot (or sample) with a single operation of the sampling device. The sample (or sub-sample) is made from the reunion of many increments ($N \geq 30$ increments recommended) taken at random locations across the lot (or sample) to be represented. Incremental sampling increases the probability of sampling each location of the lot. When used with a correct sampling device, it can provide correct sub-samples. However, the materialization error can increase the uncertainty if the increments are biased due to poorly designed sampling tools. Incremental sampling relies somewhat on the skill and experience of the sampler to avoid bias and acquire a representative sample. The sampling device must allow for correct sampling. For example in Figure 10.2 below, a scoop with a rounded bottom is not properly delimited to obtain a correct sample because it prevents one from sampling the particles at the bottom of a sample with the same probability as the particles at the top. For a correct sample, the scoop needs to have a flat bottom and parallel sides (e.g. square or rectangular).

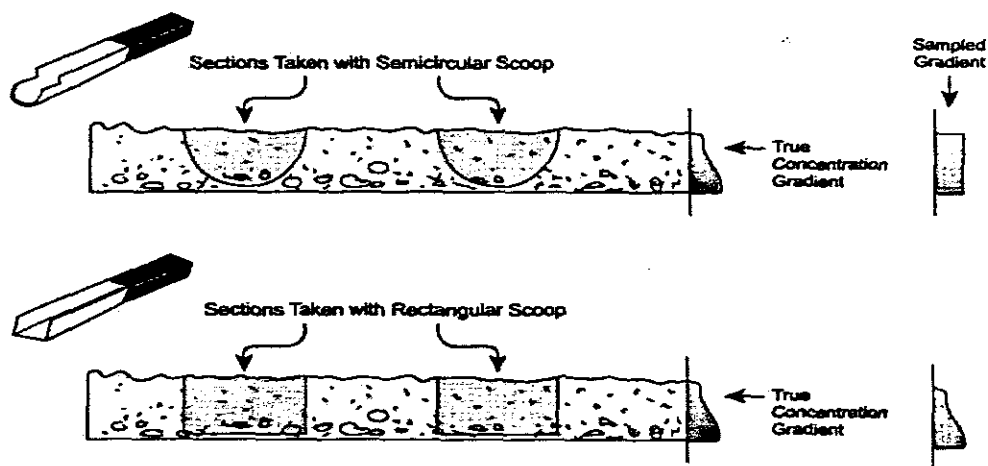


Figure 10.2: Top (increments selected with an incorrect device), Bottom (increments selected with a correct device).

To sample a one-dimensional lot (Pitard, 1993; p 239), form the material into an even long pile made from many layers (the more, the better) and take at least 30 increments, each taken entirely across the pile at several equally spaced points until the sample mass, M_s , is acquired. Thus, if 30 increments are being taken to make the sub-sample, then the mass of each increment should be about $M_s/30$. Taking each increment requires a correct sampling device to remove all of the material from top to bottom in the pile. The one-dimensional pile is recommended for laboratory incremental sub-sampling. If the mass required for the sub-sample is so small that taking 30 increments is physically constraining, then fewer increments may be taken, although the error may increase with fewer increments. The relative variance due to the grouping and segregation error, S_{GE}^2 , can be made relatively small compared to the relative variance due to the fundamental error, S_{FE}^2 , by increasing the number of random increments, N . At least $N = 30$ increments are recommended as a rule of thumb to reduce S_{GE}^2 compared to S_{FE}^2 (Pitard, 1993, p187). Grinding the sample or using a sectorial splitter may be a better option in this case.

To sample a two-dimensional lot (Pitard, 1993, p230), form the material into a flat pancake and take at least 30 increments at random locations using a cylindrical sampler with a constant cross section, with the sampler's cutter perpendicular to the pile and take the increments all of the way through the pile. Two-dimensional sub-sampling is usually not as reliable as one-dimensional incremental sub-sampling for the laboratory, since the material from the increment can easily fall back onto the sample surface, especially if the material is very dry.

Incremental sampling with at least 30 increments reduces the relative variance of the grouping and segregation error, S_{GE}^2 . However, there are few cases where this is ineffective, such as when the number of particles with high levels of analyte is small. In this case, incremental sub-sampling is about as effective as taking the entire sub-sample at one spot. Each increment is still subject to the materialization error (ME). For incremental sampling, one must use a correct sampling device that minimizes this error (for example, Figure 10.2).

9.3. Riffle splitting

A riffle splitter consists of a series of alternating chutes that deposit one-half of a sample into one discharge bin and the other half into a second bin (Figure 10.3). The method is limited to free flowing samples. Riffle splitters utilize multiple fractions (chutes), increasing the

number of increments on each round, more so than methods such as coning and quartering. However, riffle splitters have much larger increments than sectorial splitters. Several varieties of riffle splitters have been developed. They are available in many sizes and some provide splitting of a sample into more than halves, such as fourths or eighths, in one operation.

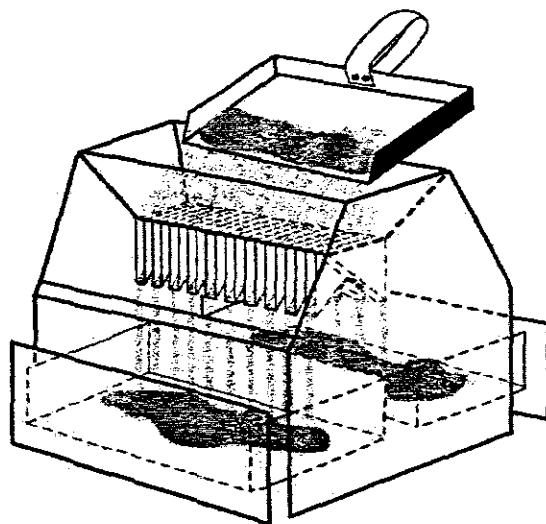


Figure 10. 3: A riffle splitter with 20 chutes and two collection pans

Riffle splitters can perform well, but the results rely on the skill and training of the operator. The sample needs to be presented to the riffle splitter such that each chute gets a similar amount, and there should be no bias in presenting the sample to the chutes (Pitard, 1993). When properly run, riffle splitters are excellent mass reduction tools.

While riffle splitters may have only 10 to 30 chutes, depending on the size and model, repeated passes result in each chute receiving particles from additional locations in the original sample. This causes the number of increments to be much larger than the number of chutes for the portion of the sample being processed. However, since one discards one-half of a sample in the first stage of a multiple-step mass reduction procedure, the grouping and segregation error associated with the first pass may dominate the uncertainty associated from the entire splitting process. This means that there may be very little improvement in reducing the grouping and segregation error after the first pass as the rest of the sample splitting procedure takes place.

9.4. Alternate shovelling

Alternate shovelling involves taking a series of scoops (increments) selected randomly from the entire sample and depositing the alternate scoops in two piles containing an equal number of scoops (Figure 10.4).

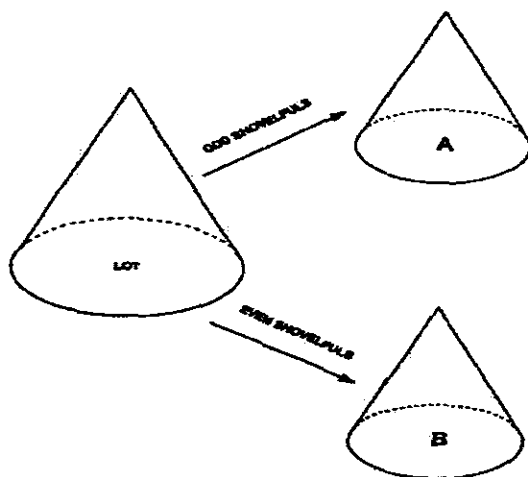


Figure 10. 4: The alternate shoveling procedure

The increments should be the same size and the minimum number of increments should be around nine for each pile. However, increasing the number of increments should minimize the effect of grouping and segregation error. Each scoop tends to select particles adjacent to each other, maintaining much of the naturally occurring grouping and segregation error. The analyst must balance the extra time required for small scoop sizes to achieve a lower grouping and segregation error with being able to accomplish all the shovelling steps in the time available for sample processing. Another drawback with this method is that the procedure may need to be repeated until the sample is reduced to the mass required for chemical or physical analysis.

9.5. Coning and quartering

Coning and quartering involves mixing and then pouring the sample into the shape of a cone (Figure 10.5). The cone is flattened, divided into four sections with a cross cutter having 90° angles, or by first cutting it in half with a stiff piece of material (e.g. sheet of plastic or paper), and then dividing each half to get quarters. Alternate quarters (splits) are combined to make a sub-sample, and one sub-sample is chosen at random for any additional mass reduction until

the desired sub-sample mass (M_s) is reached. As with alternate shovelling, this method can take considerable time to obtain a sub-sample.

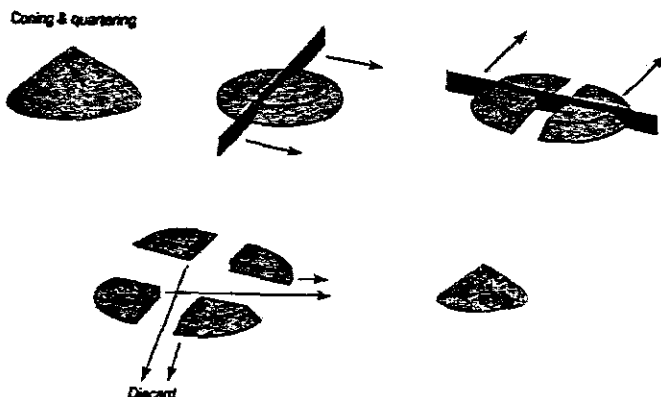


Figure 10. 5: The coning and quartering procedures

Coning and quartering is a process that preserves particle correlations within each quadrant, and this effect is worsened by combining quarters. Essentially, one has obtained a two-increment sample containing one-half of the original mass. Thus, there is some tendency to maintain the variability due to grouping and segregation problems. In coning and quartering, there is also the difficulty of increasing the initial pile so that all of the particles are randomly distributed across each quadrant. Coning and quartering is not recommended since it is a lot of effort just to reduce the grouping and segregation error by two (the number of increments, $N = 2$) each time that the method is performed.

9.6. Rolling and quartering

Rolling and quartering is variation on coning and quartering. The sample is placed in a conical pile on a large sheet of material with a smooth surface, such as glazed paper, a thin plastic sheet, or rubberised cloth. The cone is then flattened and the material is mixed by rolling it back and forth. The material is returned to the centre by lifting all four corners of the sheet, flattened out, and then split in half using the quartering procedure. One-half of the material is selected at random for any further mass reduction or for analysis.

The only difference between this method and coning and quartering is that some mixing takes place when the sample is rolled. This activity will cause any loosely bound clumps of particles to break apart. It may also serve to reduce some bias in the sample pile associated

with pouring out the sample. Overall, there is little difference between rolling and quartering, and coning and quartering. Therefore, this method cannot be recommended either.

9.7. Fractional shovelling

Fractional shovelling involves processing the sample into several sub-samples. One increment (shovel-full or scoop-full) of material at a time is removed from the lot or sample (as a pile) and added in turn to form each of the sub-sample piles (Figure 10.6).

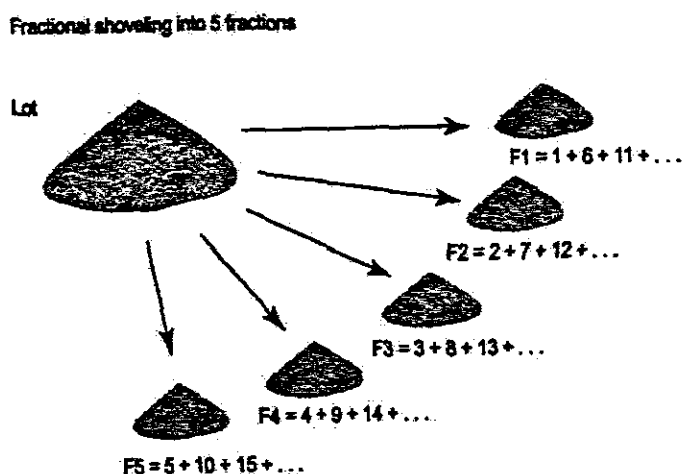


Figure 10. 6: The fractional shovelling procedure

This method has characteristics very similar to alternate shovelling and the minimum number of increments should be 10 per pile. In this case, the sample is divided into several piles. The number of increments will be inversely related to the number of sub-sample piles and to the particle correlation level. Once the original lot or sample pile is exhausted, one of the new sub-sample piles is selected at random. If the sub-sample pile is still too large (greater than M_s), then it can be reduced with another round of fractional shovelling, and the process can be repeated until the desired sub-sample mass (M_s) is obtained.

Fractional shovelling can be time-consuming for large samples. In addition, segregation effects related to density may result in trends in composition as the pile is reduced. For small samples, this may result in an increased bias between piles, as the last increment may be enriched (or depleted) compared to previous increments. If the resulting piles do not appear to be visually similar, then the sample characteristics may not be amenable to splitting by fractional shovelling.

9.8. Degenerate fractional shovelling

Degenerate fractional shovelling is similar to fractional shovelling. The only modification is that one out of every so many (e.g. every fifth scoop) increments is placed in the sub-sample pile while the other scoops are placed in a discard pile (Figure 10.7).

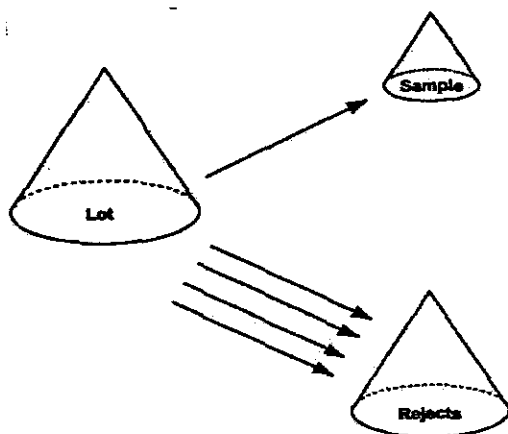


Figure 10. 7: The degenerate fractional shoveling procedure

Degenerate fractional shovelling is expected to perform slightly worse than fractional shovelling, as the operator has only one pile designated for a sub-sample. This situation lends itself to deliberate or unintended bias when choosing part of the sample with the scoop. This makes degenerate fractional shovelling a biased method and it should be avoided.

For fractional shovelling methods, the variability from the grouping and segregation error will increase with larger, but fewer, increments (scoop sizes), and the variability will increase with a larger number of sub-samples (containing fewer increments) considered at a time. For example, if there are just two sub-samples, then only 50% of the sample can be selected each time, and subsequent sub-sampling is expected to select portions from any of those sub-samples for final analysis. However, for 10 sub-samples, or 1/10 degenerate fractions, the operator discards 90% of the sample. If a second phase of sub-sampling is carried out, then only 10% of the original material is available at the beginning of the second phase; thus, much of the grouping and segregation error from the first phase will remain and could influence the overall error from the remaining sample reduction steps. That is, whatever bias was introduced at the first stage will most likely influence all of the subsequent steps of the sample mass reduction process. This type of problem is similar to the one discussed for riffle splitters.

9.9. Table sampler

A table sampler consists of an inclined surface with various triangular prisms placed to divide the sample as the surface is vibrated and the particles move from the top to the bottom (Figure 10.8).

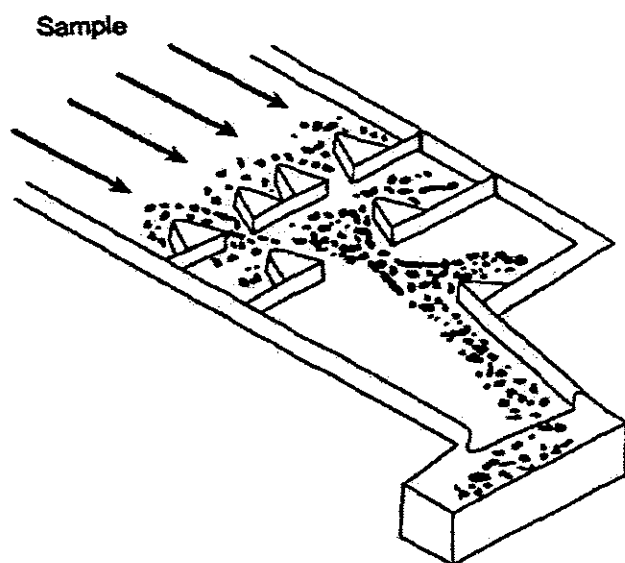


Figure 10. 8: A table sampler

Like the riffle splitter, this device splits the sample in one pass. However, the number of increments associated with this technique is small with a tendency to allow large grouping and segregation errors to remain. The device is also bulky and not readily available. This method has little to offer for recommendation. The method should suffer from operator bias in pouring the sample into the apparatus in the same manner that degrades the performance for coning and quartering, and for riffle splitting. The initial location on the table with respect to the other parts of the sample will bias certain particles toward a particular sub-sample. In effect, some of the initial correlation derived from the placement of the sample is maintained, and that means that some of the grouping error is maintained.

9.10. V-Blender

V-blenders are devices for homogenizing samples (Figure 10.9). However, the material in a V-blender tends to segregate in the time it takes to discharge the sample, and the material will most likely segregate again as it is discharged from the bottom of the blender. Obtaining

unbiased sub-samples using this method would require “correct” sampling practices prior to discharging the material from the blender.

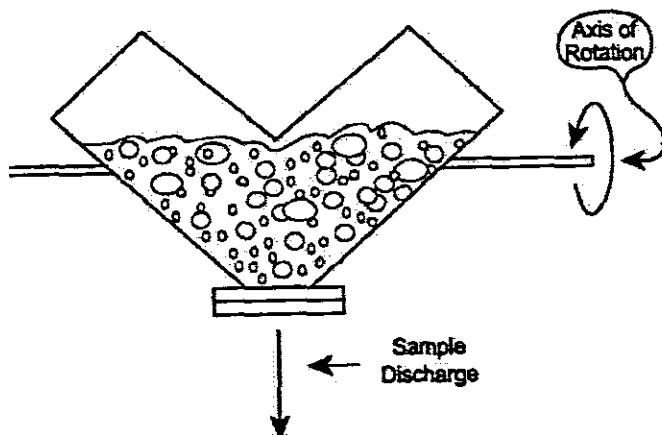


Figure 10. 9: A V-blender

9.11. Vibratory spatula

This device is sometimes used to feed material when dividing samples. Its use should be avoided. The result is more likely to enhance segregation than to reduce it. It is well known that vibrating a quantity of particles tends to enhance segregation based on size, shape and weight.

9.12. Grab sampling

Grab sampling almost always involves taking the sub-sample off the top of the sample. One or more scoops are typically placed on a balance. The scoop, most likely an incorrectly designed sampling device, is often used to return some of the material to the sample container if the mass is larger than needed for the analytical procedure. Grab sampling does not meet the criteria of a correct sampling procedure for heterogeneous particle because it does not give each particle the same probability of being sampled. Grab sampling does absolutely nothing to reduce the sampling errors that can be minimized through correct sampling techniques. If the analyte is associated with particles that have physically different characteristics such as size, shape or density, then a biased result is expected. If there is tendency for the particles to segregate, then the bias and uncertainty may be very large. Grab sampling is particularly prone to generating biased results due to gravity effects and to sampler bias.

Grab sampling is judgemental and non-probabilistic, and should be avoided since it is not designed to take a representative sub-sample. As a sampling method, the grab sampling procedure appears to be designed to provide biased results. Grab sampling should only be considered if one has previously shown that the matrix and particle size have no significant effect upon sampling error. Even then, the analyst is at risk of reporting unreliable results if any of the samples fail to meet those assumptions.